THE CONTRIBUTION OF HIGHWAY TUNNELS TO AIRBORNE PARTICLE CONCENTRATIONS IN AN URBAN AREA

A Senior Honors Thesis

by

Jennifer Skerker
B.S. Environmental Engineering, 2017
Tufts University, School of Engineering,
Department of Civil and Environmental Engineering

Advisor: Professor John Durant

Abstract

Over the past twenty years, the urban landscape of Boston, MA has been transformed as a result of the "Big Dig," a multi-billion dollar project that replaced the aboveground Central Artery highway in Boston with an underground highway. With the completion of this project, the city of Boston has forty-five new public parks and plazas, and a 62% total reduction in vehicle-hours of travel on I-93 from 1995 to 2003; however, there has not been much research on characterizing the extent to which vehicle-related air pollution patterns have changed. The purpose of this research is to better understand spatial and temporal, tunnel-related pollution patterns in Boston for particulate matter less than 2.5 microns in diameter ($PM_{2.5}$) from the Central Artery/Tunnel (CA/T). Mobile pollution data through the CA/T and EPA stationary-site data in and around Boston were analyzed to understand $PM_{2.5}$ spatial and temporal patterns. Modeling was completed in AERMOD, a steady state Gaussian dispersion model developed for industrial point sources. Measurements at EPA stationary-site monitors showed that $PM_{2.5}$ concentrations were below the National Ambient Air Quality Standards, even in downtown Boston. About one-third of ambient $PM_{2.5}$ concentrations may be attributed to local sources. Modeling results showed that 14 to 19% of $PM_{2.5}$ concentrations may come from tunnel-related sources; however, this is highly dependent on the emission factor used. $PM_{2.5}$ concentrations do not vary much seasonally or weekly. $PM_{2.5}$ concentrations in the Boston area are greatest when winds are from the southwest. Although the local mobile component of $PM_{2.5}$ is small compared to regional sources, it still impacts ambient $PM_{2.5}$ concentrations in Boston.

1.0 Introduction

1.1 Transportation Changes in Boston

Over the past twenty years, the urban landscape of Boston, MA has been transformed as a result of the "Big Dig," a multi-billion dollar project that replaced the aboveground Central Artery highway in Boston with an underground highway. The purpose of this project was to reduce traffic in Boston, as traffic on Interstate 93 (I-93) often persisted for upwards of ten hours per day, and the accident rate on the highway was four times the national average for urban interstates (Massachusetts Department of Transportation, 2017a). Prior to the "Big Dig," I-93 ran entirely aboveground; since the "Big Dig," about 2400 meters of the highway runs underground through central Boston in the Thomas P. O'Neill Jr. Tunnel ("Central Artery/ Tunnel") (Massachusetts Department of Transportation, 2017b). With the completion of this project, the city of Boston has forty-five new public parks and plazas, and a 62% total reduction in vehicle-hours of travel on I-93 from 1995 to 2003 (Massachusetts Department of Transportation, 2017a); however, there has not been much research on characterizing the extent to which vehicle-related air pollution patterns have changed.

The Community Assessment of Freeway Exposure and Health (CAFEH) study is an interdisciplinary research project that aims to better understand the relationship between traffic-related air pollutants and exposure in communities near highways and major roadways (Fuller et al., 2012), with a focus on I-93. Emission factors (EFs) for ultrafine particulates (UFPs; diameter less than 100 nanometers) and nitrogen oxides (NO_x) from data collected within the Central Artery/ Tunnel (CA/T) have been estimated using a mobile monitoring laboratory (Perkins, Padró-Martínez, & Durant, 2013). However, no location-specific EFs for particulate matter less than 2.5 microns ($PM_{2.5}$) have been developed. Limited modeling work has been completed to

understand the spatial and temporal distribution of emitted pollutants from the tunnel and what communities, if any, could be at risk from elevated pollution levels.

With the creation of the underground tunnel, the CA/T, as a source of pollution, has been transformed from a line source to several point sources at the exits. As a result, the pollution is emitted at fewer locations, but at more concentrated levels at those sites. The modeling work that has been done ensured that air quality levels were below the national ambient air quality standards (NAAQS). Since the creation of the CA/T, a permit must be renewed every five years to continue to emit pollution from the tunnel. In the operating certification for the tunnel, modeling of the criteria air pollutants has been done using the American Meteorological Society/ Environmental Protection Agency Regulatory Model (AERMOD) (TRC/Parsons Brinckerhoff, 2012). In the operating certification model, the pollutant sources were considered to be the transverse vents from the ventilation system and the longitudinally ventilated exit ramps. Ventilation Building #4 (VB #4) includes four stacks, and is about 500 meters from the exit of the CA/T northbound bore (Figure 1) (TRC/Parsons Brinckerhoff, 2012). This operating certification did not include the two main tunnel exit portals as pollutant sources, which, along with ventilation systems, also have an effect on the air quality in the surrounding area (El-Fadel & Hashisho, 2001).

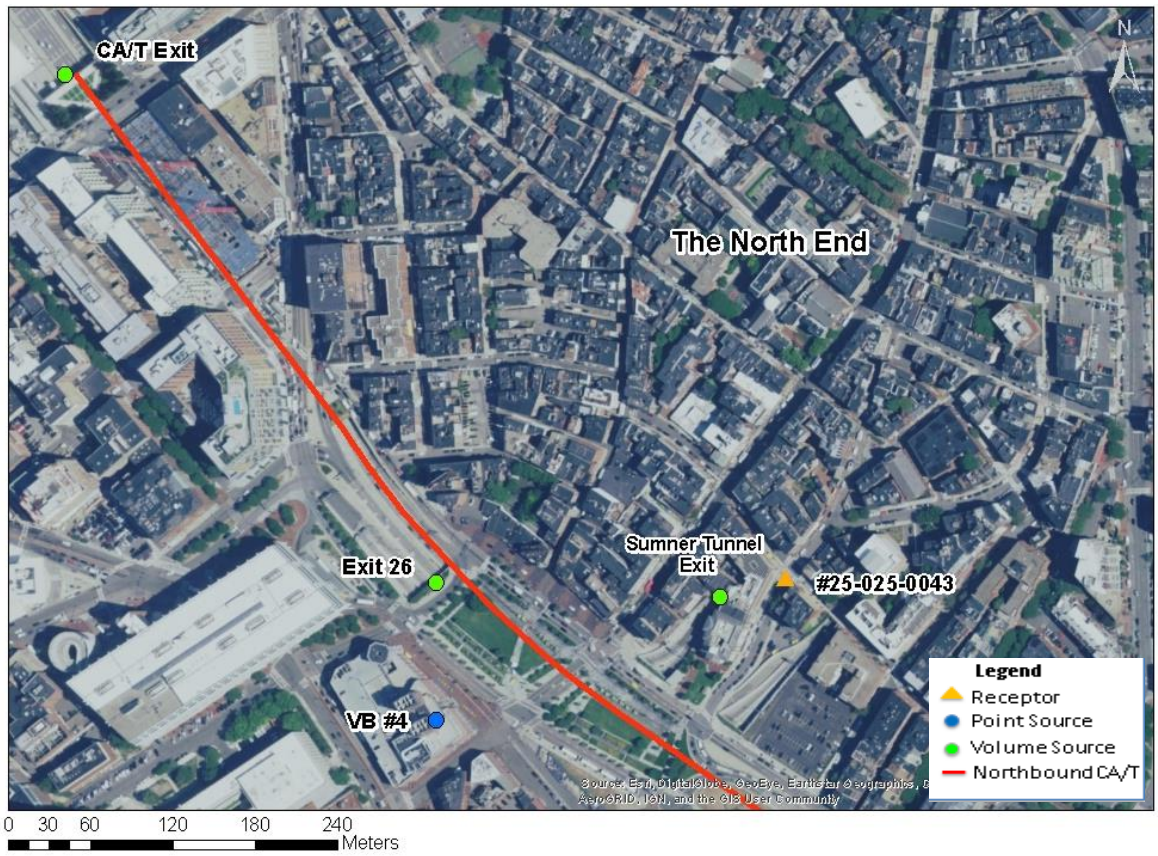

Figure 1. A Map of the Sources Analyzed in AERMOD and the Proximity of the Sources to the North Street EPA Monitoring Site (#25-025-0043).

The purpose of this thesis is to better understand tunnel-related spatial and temporal patterns in Boston for $PM_{2.5}$. By understanding how the CA/T has changed dispersion patterns, better-engineered solutions may be designed to inhibit local exposure and improve public health.

1.2 Health Effects of $PM_{2.5}$

Research over the past decades has shown that traffic-related particulate matter plays an important role in urban air pollution (Engel-Cox & Weber, 2007; Lee et al., 2011b; Valavanidis et al., 2008). Particulate matter is frequently categorized by size, which plays a role in how far particles may penetrate into the human body (Valavanidis et al., 2008). By convention, particulate matter is divided into particles less than ten microns (PM_{10}), less than 2.5 microns

($PM_{2.5}$), and less than 0.1 microns (UFPs). As particles decrease in size, they make up a smaller proportion of the total mass concentration of pollutants, but increase in number concentration and have a higher surface area to mass ratio that contributes to how the particles aggregate and interact with biological systems (MacNee & Donaldson, 2003).

Smaller particles can penetrate further into the lungs and have been hypothesized to cause alveolar inflammation, which can then cause changes in blood coagulability leading to a greater susceptibility for cardiovascular disease (Harrison & Yin, 2000; Seaton et al., 1995). As a result, $PM_{2.5}$ can have significant health effects such as increased rates of cardiovascular, cardiopulmonary, and respiratory diseases (Bates, 1992; Franchini & Mannucci, 2007; Riedl, 2008; Valavanidis et al., 2008).

1.3 $PM_{2.5}$ Concentrations in Tunnels

Multiple studies around the world have taken measurements throughout vehicle tunnels or at the inlet and outlet. Results have shown that $PM_{2.5}$ concentrations at the exit are higher than $PM_{2.5}$ concentrations at the entrance, and that measured concentrations are much higher than $PM_{2.5}$ standards in the United States. Assuming conservation of mass, this data has been used to determine emission factors (Cheng et al., 2006; Weingartner et al., 1997; Zhou et al., 2014). Exit and entrance $PM_{2.5}$ concentrations varied by factors ranging from 4.86 on a Sunday to 8.07 on a workday and an exit concentration of 201.6 $\mu g/m^3$ was measured in the Gubrist Tunnel in Zürich, Switzerland (Weingartner et al., 1997). The average exit $PM_{2.5}$ concentration at the Shing Mun Tunnel in Hong Kong from the DustTrak was 260.0 ± 136.4 $\mu g/m^3$ (Cheng et al., 2006). The peak concentration during morning rush hour traffic in the Xiangyin Tunnel in Shanghai, China was 468.45 $\mu g/m^3$ (Zhou et al., 2014). In the M5 Tunnel in Sydney, Australia, when the cabin

windows were down, average $PM_{2.5}$ concentrations were 388 μg/m^3, with a peak of 526 μg/m^3 (Cains et al., 2003). In comparison, the NAAQS primary and secondary, 98th percentile, 24-hour standard is 35 μg/m^3 (US EPA, 2016a).

1.4 Modeling the Air Quality Impacts of Tunnels on Surrounding Areas

There are four common types of tunnel studies: (1) studies that use vehicle tunnels to determine EFs, assuming conservation of mass (Colberg et al., 2005; Deng et al., 2015; Gillies et al., 2001; Grieshop et al., 2006; Perkins et al., 2013); (2) empirical studies that involve physical, scaled models in wind tunnels to better understand various wind, dimension, and dispersion characteristics (Balczo et al., 2011; Lepage et al., 1997; Oettl, 2015; Perry et al., 2016); (3) studies that use models, such as dispersion models or numerical simulations, to understand the processes within tunnels (Chung & Chung, 2007; Eftekharian et al., 2014; El-Fadel & Hashisho, 2001; Gao et al., 2004; Gidhagen et al., 2003); and (4) studies that use dispersion models and measurements to look at tunnel portals and vents as sources for local pollution levels (El-Fadel & Hashisho, 2001; Miao & Fu, 2013; Okamoto et al., 1998). This research focuses on the modeling and measurements of tunnel portals and vents as local pollution sources.

Research on the modeling and measurements of tunnel portals and vents as local sources is important because currently, cities, such as Boston, MA; Stockholm, Sweden; and Antwerp, Belgium have built or are planning to build roadway tunnels in urban areas to replace crowded, elevated roads and improve air quality. Although these replacements improve air quality in areas where roads are removed, they may have the unintended consequences of increasing pollution levels in areas near tunnel portals and ventilation systems, as well as within tunnels (Brusselen et al., 2016; Orru et al., 2015). In Brusselen et al. (2016) where $PM_{2.5}$ and NO_2 concentrations were

explored for a future tunnel project in Antwerp, the researchers calculated that the tunnel would improve the air quality for about 352,000 people and worsen the air quality for 15,366. Although 15,366 people is a small percentage of 352,000 (4.4%), the study concluded from a public health perspective that it is not acceptable to worsen the air quality for this number of people (Brusselen et al., 2016). This study recommended moving the tunnel portals farther away from densely-populated areas (Brusselen et al., 2016).

Many different models have been used to analyze the air quality effects from different tunnels. Empirical models have been developed for specific tunnels, but are usually unable to be applied to different tunnels (Nadel & Vanderheyden, 2000; Oettl et al., 2002). Two models have been developed specifically for modeling the dispersion of tunnel portals (Oettl et al., 2003). One model, Grazer Lagrange model, is a Lagrangian model that uses a stochastic process to estimate the concentrations of air pollutants. In this model, exit velocity, buoyancy, and traffic induced turbulence are taken into account; additionally, the flow field is developed through horizontal streamlines and vertical mixing from a modified version of Van Dop's model (Oettl et al., 2002). The other model is the JH-model, a Gaussian dispersion model that contains two modules: a wind field model called MASCON, which combines the interpolation of observational data with wind flow from the tunnel portals, and a diffusion module using a one-dimensional Taylor-Galerkin scheme (Oettl et al., 2003). The Taylor-Galerkin scheme is a numerical method that was chosen to solve the advection equation (Okamoto et al., 1998). The main application of these models has been in analyzing tracer gases to understand dispersion patterns, rather than specific vehicle-related pollutants.

Other studies have used different Gaussian models to analyze the nearby pollutant concentrations from tunnel portals. In Ginzburg and Schattanek (1997), portal jet plumes exiting

from the tunnel were modeled as volume sources. The length of the volume source depends on the flow of traffic, tunnel ventilation, and meteorological wind conditions (Ginzburg & Schattanek, 1997). In analyzing the impacts of a future tunnel project in Stockholm, Sweden, the Airviro air quality management system, which includes a Gaussian dispersion model, compared two different scenarios: one with the current above-ground highway and the other with a proposed 18-kilometer tunnel bypass. The main difference in the tunnel bypass scenario was that the sources relating to vehicle-traffic on the road were ventilated towers and the tunnel exits. Modeling showed that ground-level concentrations from the ventilation towers were very low compared to ground-level concentrations from the tunnel exits (Orru et al., 2015). In order to look at the effects of complex terrain on pollutant dispersion, Balczó et al. (2011) used a computational fluid dynamics model. This study looked at the effects of topography, vegetation, and buildings on pollutant concentrations by comparing wind tunnel test data to the modeled data. This study concluded that air quality limit exceedances from tunnel portals could be avoided through the addition of ventilation stacks (Balczo et al., 2011).

Recent studies have also used hybrid models for better understanding $PM_{2.5}$ dispersion more generally in urban areas. For example, Michanowicz et al. (2016) modeled $PM_{2.5}$ using AERMOD and a land use regression (LUR) to determine the temporal variation over the course of a year and spatial variation over 500 km^2 around the Pittsburgh metropolitan area. This study found that LUR outperformed AERMOD predictions, but that using AERMOD outputs as LUR inputs improved the accuracy of predictions by 2 to 10 percent (Michanowicz et al., 2016). Another study combined AERMOD with the Community Multiscale Air Quality (CMAQ) grid model to determine more accurate total ambient concentrations (Cook et al., 2008). In Isakov et al. (2014), local source contributions of carbon monoxide, NO_x, and $PM_{2.5}$ were determined

through the CMAQ model and the Space/Time Ordinary Kriging model, and urban background contributions were determined through AERMOD and the Research LINE-source dispersion model for near-surface releases (RLINE). AERMOD was used to estimate stationary sources, and RLINE was used to estimate emissions near roadways (Isakov et al., 2014). AERMOD has also been used on a regional scale to model $PM_{2.5}$ from traffic-related sources, which showed that population exposure to $PM_{2.5}$ can be estimated accurately for smaller scales as the area modeled was 12,000 km^2 (Rowangould, 2015).

Prior to the construction of tunnels, dispersion models and/or physical wind tunnel models are frequently developed to predict concentrations in and around portals; the goal of these models is to ensure that concentrations will not surpass regulated levels. In the U.S., air pollution levels are regulated by the NAAQS (US EPA, 2016a). Prior to the construction of the CA/T in Boston, a physical, to-scale wind tunnel was constructed and analyzed. In this analysis, eight of the eleven exit ramps met the air quality standards. The three exit ramps that did not meet the air quality standards were all located close to then present or planned buildings, and so the receptor was close to the exit ramp and the surrounding space was very confined, limiting dispersion. (Lepage et al., 1997)

1.5 Spatial and Temporal Trends in $PM_{2.5}$

Measurement campaigns have shown that $PM_{2.5}$ concentrations tend to be higher in the summer and the winter than in the fall and spring; however, studies in the Northeast United States have shown conflicting results on if concentrations are higher in warm or cold seasons (Bell et al., 2007; Lee et al., 2011a). In data collected from the Boston Metropolitan Area between 2009 and 2012, $PM_{2.5}$ concentrations increased with greater temperatures (Patton et al., 2014). Conflicting

results from various studies may result because different sources of pollution emit different amounts seasonally; for example, the contribution of $PM_{2.5}$ from motor vehicles was statistically higher in the winter (Lee et al., 2011a). Another reason may be that different temperatures produce different chemical reactions, further impacting the composition of $PM_{2.5}$ (Bell et al., 2007).

Average daily $PM_{2.5}$ concentrations in New England typically ranged from 9.0 to 17.0 $\mu g/m^3$ in two studies conducted between 2000 and 2004 (Lee et al., 2011a; Lee et al., 2011b). Annual $PM_{2.5}$ concentrations exhibit a general downward trend (McGrath et al., 2016), and at the $PM_{2.5}$ Federal Reference Method (FRM) monitoring sites in Massachusetts for 2015, the annual average concentrations ranged between 5.11 and 7.55 $\mu g/m^3$ and the 98^{th} percentile, 24-hour measurements ranged between 13.0 and 19.4 $\mu g/m^3$. The NAAQS for average annual $PM_{2.5}$ concentration and the 98^{th} percentile, 24-hour $PM_{2.5}$ concentration are 12.0 and 35.0 $\mu g/m^3$, respectively (McGrath et al., 2016).

1.6 Goals and Objectives

The purpose of this thesis is to better understand spatial and temporal patterns of tunnel-related $PM_{2.5}$ in Boston. The first objective is to understand $PM_{2.5}$ patterns within the Central Artery/Tunnel, and the possible impacts on dispersion from the tunnel. The second objective is to identify spatial and temporal patterns for $PM_{2.5}$ concentrations at the North Street monitoring site (#25-025-0043) and then to compare the data to background sites outside of Boston proper. The last objective is to create a model of $PM_{2.5}$ dispersion patterns in AERMOD to better understand if model results can predict $PM_{2.5}$ concentrations.

2.0 Methods

2.1 Mobile Monitoring Data Collection and Preparation

Mobile monitoring data was collected as described in Perkins et al. (2012) using the Tufts Air Pollution Monitoring Laboratory (TAPL). The TAPL is a mobile monitoring lab with rapid-response instruments to measure multiple pollutants (Padró-Martínez et al., 2012). The data analyzed were collected between December 2011 and November 2013 on 42 dates. One date was removed because all measured $PM_{2.5}$ concentrations were below the detection limit at the same concentration, most likely meaning that the instrumentation was not working properly on that day. No other data was removed. Of the 41 remaining dates, 12 were in the Fall, 13 in the Winter, 9 in the Spring, and 7 in the Summer. 15 tunnel runs were in the morning, 22 were in the afternoon (between 12 and 6 PM), and 4 were in the evening (after 6 PM). 33 tunnel runs were on weekdays and 8 were on weekends. The data was aggregated into one spreadsheet by time. $PM_{2.5}$ was collected using a laser photometer (Sidepak AM510, TSI). The instrument had a detection limit of 1.0 $\mu g/m^3$ and recorded data every ten seconds (Padró-Martínez et al., 2012). The $PM_{2.5}$ measurements were multiplied by a factor of 0.6 to take into account the density of particulate matter found in Boston (Masri et al., 2015).

The first step in preparing the data was to divide the file for each date of data collection in two to separate TAPL runs through the northbound and southbound tunnel bores. Data from within the CA/T tunnel were easily identifiable because the GPS receiver lost signal in the tunnel, so most of the tunnel data is missing GPS coordinates. Data missing GPS signals was filled in with the GPS coordinates directly before the GPS receiver lost signal for use in Geographic Information Systems through ArcMap.

MassDOT Roads layers were uploaded into ArcMap as background and for use in identifying exactly what mobile measurements took place in the tunnel (MassGIS, 2014; The Massachusetts Department of Transportation- Office of Transportation Planning, 2014). The specific roads that make up the northbound tunnel route were selected in ArcMap, and a new shapefile was created and exported from this; the same process was repeated for all tunnel routes that the TAPL followed. Three tunnel routes were analyzed: the northbound tunnel route; the southbound tunnel route entering on I-93 and exiting about 1200 meters through the tunnel onto Purchase Street (Exit 23); and the southbound tunnel route entering via I-93 and exiting towards I-90 onto Albany Street (Exit 20-B). The data on each date was divided and sorted by route. The TAPL data was imported to ArcMap using the latitude and longitude coordinates. The data points were then snapped to the specific tunnel road layer to isolate data within about 500 meters of the tunnel. Only the northbound tunnel bore data was further analyzed.

2.2 EPA Monitoring Data

Stationary-site data were obtained from the U.S. Environmental Protection Agency (EPA) Air Data database (US EPA, 2016b). Data were compared between sites in and around Boston, mainly focusing on the North Street EPA site in Boston, Massachusetts (#25-025-0043) (Figure 2). Background sites were the EPA sites in Lynn, Massachusetts (#25-009-2006), which is 14 kilometers north-northeast of Boston, and at the Blue Hill Observatory in Milton, Massachusetts (#25-021-3003), 17 kilometers south-southwest of Boston. Both background sites were chosen because they are outside of, but close to Boston, and should therefore approximate regional $PM_{2.5}$ concentrations. The North Street site was about 640 meters southeast of the CA/T

Northbound Tunnel exit, 280 meters northeast of the CA/T Ventilation Building 4, 60 meters northeast of the Sumner Tunnel exit, and 260 meters east of Exit 26 from the CA/T (Figure 1).

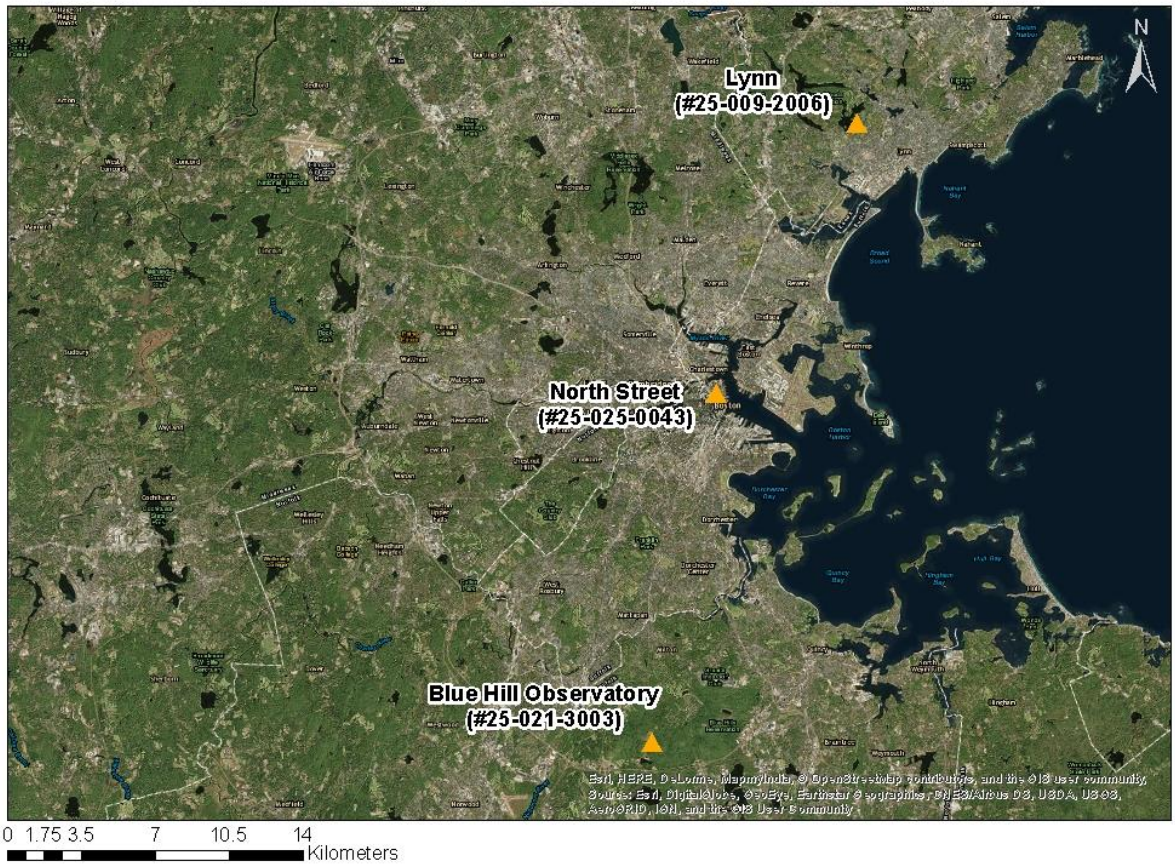

Figure 2. A Map of the EPA Stationary-Site Monitoring Sites Analyzed.

The North Street site had daily FRM and Federal Equivalence Method (FEM) data. The $PM_{2.5}$ FRM was a filter-based, gravimetric method that provides a single concentration at a 24-hour sampling interval. The mass concentration was measured through the net mass gain at the filter divided by the sample volume. At the North Street site, the FEM used was Met-One BAM-1020 W/ PM2.5 SCC, which was a continuous beta attenuation method (Code: 731). At the Blue Hill Observatory site, the FEM used was Met One BAM-1020 Mass Monitor w/VSCC, which was a continuous beta attenuation model (Code: 170) (US EPA, 2016b, 2017). The Lynn site had FRM data collected every three days.

FEM data from the Blue Hill Observatory was adjusted so that it could be compared to the FRM data. An adjustment factor was determined by finding the average value of the FRM measurement divided by the FEM measurement at the North Street site on all days that both methods were used. This factor was then multiplied by the FEM Blue Hill Observatory data. Finding the factor between the two values was chosen over finding the difference. This is because when a linear regression between the two data sets was analyzed, the values did not meet the Code of Federal Regulations (CFR) that the slope must be 1.0 ± 0.1 and the intercept must be 0.0 ± 2.0 $\mu g/m^3$ (Figure A.1) (US EPA, 2010, p. 53). The determined adjustment factor was 0.8119.

Upon examination of the data, it was found that some measured values at all three sites were less than zero. According to the CFR (40 CFR Part 58, Appendix A–E), 3 $\mu g/m^3$ is the limit for data points that can be compared between methods (40 CFR Part 58, Appendix B, Section 4) (U.S. Government Publishing Office, 2016). All values at or below 3 $\mu g/m^3$ at each site were removed from the data sets. Table 1 includes the number of values at or below 3 $\mu g/m^3$ and the number of data points remaining for use in analysis. Data from 2011 to 2015 was examined. This time period was chosen for three reasons: (1) federal regulations require modeling efforts to cover at least five years (Environmental Resources Management, 2015), (2) this time period was the most recent fully-available dataset, and (3) this timespan included the time period that the TAPL data was collected in. This data was used to compare to model results.

Table 1. The Number of Daily-Average $PM_{2.5}$ Values ≤ 3 μg/m^3 at each EPA Site from 2011–2015.

Site	Method	Total Number Measurements	Measurements ≤ 3 μg/m^3	Percentage Removed (%)	Number of Measurements Remaining
Blue Hill Observatory (25-021-3003)	FEM	1750	346	19.8	1404
Lynn (25-009-2006)	FRM	591	98	1.0	493
North End (25-025-0043)	FRM	1777	45	2.5	1732

2.3 AERMOD Model Setup and Implementation

This study used AERMOD, a steady state Gaussian dispersion model developed for industrial point sources (Cimorelli et al., 2004). AERMOD is recommended by the EPA as the "best state-of-the-practice Gaussian plume dispersion model" (US EPA, 2005). AERMOD is appropriate to use for stationary sources in simple and complex terrain (US EPA, 2005). Sources in AERMOD can be modeled as point, area or volume sources. One reason for choosing AERMOD for this modeling effort was to better understand how suitable AERMOD is for mobile sources. AERMOD uses the Monin-Obukhov length to calculate the buoyancy effects for turbulent flow (Cimorelli et al., 2004). Inputs in AERMOD include meteorological data, elevation data, and pollution source data.

Meteorological data were obtained from the National Oceanic and Atmospheric Administration (NOAA) and processed in AERMET View 9.0.0 (Lakes Environmental, 2017). Hourly surface data were obtained at Logan Airport (Station #14739) from the Integrated Surface Hourly Data Base (NOAA, n.d.). Upper air data were obtained from the NOAA Earth System Research Laboratory (ESRL) at Chatham, Massachusetts (Station #14684) (NOAA et al, 2016). Wind data were compiled using the AERMINUTE feature in AERMET using 1-Minute Automated Surface Observing System Wind Data (TD-6405).

Terrain and elevation data was obtained from a National Elevation Dataset GeoTIFF Digital Terrain File for NAD 83 obtained through the preprocessor AERMAP in AERMOD.

Four sources relating to tunnel-related vehicle emissions were input into AERMOD (Figure 1). VB #4 was modeled as a point source, since ventilation stacks emit pollution from the tunnel at that point. Three tunnel exits: the main northbound CA/T Exit, Exit 26 from the CA/T, and the Sumner Tunnel Exit (southbound bore) were all modeled as volume sources because tunnel exits plumes have length, height, and width components associated with the tunnel dimensions and cars pushing air through the tunnel. Point source parameters, such as the release height, gas exit temperature, stack inside diameter, and gas exit velocity were obtained from the modeling performed in the operating certification for the CA/T ventilation system (TRC/Parsons Brinckerhoff, 2012). For VB #4, the emission rate from the operating certification was used (0.208 grams per second). For Exit 26 and the main CA/T exit, it was assumed that 25% of the $PM_{2.5}$ emitted from the northbound bore exited at Exit and the other 75% continued to flow through the tunnel.

The volume source $PM_{2.5}$ emission rates were determined using the following equation:

$$Emission\ Rate\ \left(\frac{g}{s}\right) = EF\ \left(\frac{g}{veh*km}\right) * Cars\ \left(\frac{veh}{day}\right) * Length\ (km) * \left(\frac{1\ day}{86400\ s}\right).$$

The emission factor used was 0.052 grams per vehicle per kilometer from the Sepulveda Tunnel in Los Angeles, California (Gillies et al., 2001). After comparing emission factors from different studies (Table 2), this value was chosen because it was on the more conservative (low) end of the range and because this tunnel also has a low percentage of diesel vehicles (2.6%), similarly to the CA/T, which has about 3.7% diesel vehicles in the southbound tunnel and 2.5% in the northbound tunnel (*NAVTEQ Traffic*, 2012). The number of cars per day for the main northbound CA/T exit was estimated to be 88,000 (Central Transportation Planning Staff

Geoserver, 2012); for the Exit 26 emission rate, the number of vehicles per day from the CA/T was 20,500 vehicles per day, as estimated from 2010 (Central Transportation Planning Staff, 2011); and for the Sumner Tunnel in 2013, 9.4 million cars were counted at a toll, averaging to 25,700 cars per day (Massachusetts Department of Transportation, 2013).

Table 2. Literature Review of $PM_{2.5}$ Emission Factors from Vehicle Tunnel Studies.

Tunnel	**Location**	**Time Period**	**Vehicle Fleet Composition**	**EF Avg.(SD) (g/(km*veh))**	**Study**
Sepulveda Tunnel	Los Angeles, CA	July 23,1996-July 27, 1996	2.6% diesel	0.052(0.027)	(Gillies et al., 2001)
Caldecott Tunnel	San Francisco, CA	Summer 1997	0.3 to 4.8% HD diesel	0.11(0.01) for LD, 2.5(0.2) for HD	(W. Kirchstetter, Harley, Kreisberg, Stolzenburg, & Hering, 1999)
Tuscarora Mountain Tunnel	Pennsylvania Turnpike, PA	May 18, 1999-May 23, 1996	10% to 90%	0.062(0.042)	(Gertler et al., 2002)
Shing Mun Tunnel	Hong Kong	Summer and Winter 2003	50% diesel, 41% gasoline, 9% LPG	0.257(0.031)	(Cheng et al., 2006)
Kaisermühlen Tunnel	Vienna, Austria	April and May 2005	9.6% HD	0.026(0.001)	(Handler et al., 2008)
Squirrel Hill Tunnel	Pittsburgh, PA	Nov-02	19.2(2.1)%	0.158(0.029) (high-speed)	(Grieshop et al., 2006)
			11.0(1.6)%	0.189(0.023) (low-speed-rush hour)	
			36(8)%	0.437(0.076) (high truck- early morning)	

Output values in AERMOD were calculated at receptors, which have x- and y-coordinates, as well as terrain elevations (z-coordinates). AERMOD can generate average concentrations over a user-specified time period at a given receptor or can determine maximum values over a certain time period. In order to compare model results to measured data, the main receptor analyzed was the North Street EPA site (42.3631°N, -71.0541°W).

2.4 AERMOD Scenarios

Since winds mainly come from the west in Massachusetts (the southwest in the summer and the west-northwest in the winter) (Figures A.2–A.4), two scenarios were analyzed based on winds coming from the southwest and the northwest. In the first scenario, winds were analyzed at 240 (± 20) degrees (at least 40% of the hours fell within this range), since that is the approximate bearing of the Sumner Tunnel exit and VB #4 to the North Street receptor. Twelve time periods (four were in the winter, one was in the spring, four were in the summer, and three were in the fall) totaling 51 days were analyzed. In the second scenario, winds were analyzed at 300 (± 20) degrees (at least 40% of the hours fell within this range), since that is the approximate angle for emissions from the CA/T northbound exit to be measured at the North Street receptor. Nine time periods were identified (three were in the winter, three were in the spring, one was in the summer, and one was in the fall) totaling 46 days.

In order to determine time periods when the wind direction for at least 40% of the hours was coming from these two directions plus or minus twenty degrees, a wind direction time series plot was first used. Time periods had to be at least three days in length, with at least 20% of the hourly values within a 20-degree range around 240°, 30% of the hourly values within a 30-degree range around 240°, and 40% of the hourly values within a 40-degree range around 240°. This gave ranges from 230–250 degrees, 225–255 degrees, and 220–260 degrees.

2.5 AERMOD Output

Once the input requirements were satisfied, each scenario (n=60) was run in AERMOD (Table 3). The results obtained were daily, 24-hour concentrations for each date. These values were then compared with the daily differences measured between the North End FRM data and the Blue

Hill Observatory adjusted data. Modeled conditions were analyzed for all four sources, all sources but the CA/T Exit, and all sources but the Sumner Tunnel Exit. Therefore, twelve time periods were run under three different assumptions on the source contribution for the southwest winds scenario (n=36), and eight time periods were run under the same three assumptions for the northwest winds scenario (n=24).

Table 3. Modeling Scenarios Analyzed in AERMOD

				Modeling Conditions		
Scenario	Wind Direction (°)	Number of Time Periods	# Days	Four Sources	No Sumner Exit	No CA/T Exit
Southwest Winds (Mimics Summer)	240	12	51	X	X	X
Northwest Winds (Mimics Winter)	300	8	46	X	X	X

2.6 AERMOD Sensitivity Analysis

Parameters in AERMOD were varied to understand what factors had the greatest influence on modeled $PM_{2.5}$ concentrations. One time period was analyzed for each wind scenario: 2/9/2011–2/14/2011 (6 days) for southwest winds, and 1/14/2011–1/24/2011 (10 days, no data for 1/18/2011) for northwest winds. The modeling conditions analyzed included the comparison of high and low EFs from the literature, the comparison of varying percentages for the amount of pollutant exiting the CA/T Exit compared to Exit 26, and the comparison of the amount of cars passing through each exit. Additionally, the calculated EF of VB #4 was compared to the value used from the CA/T operating certification (TRC/Parsons Brinckerhoff, 2012).

For the comparison of EFs, literature values of 0.189 grams per vehicle per kilometer (Grieshop et al., 2006) and 0.026 grams per vehicle per kilometer (Handler et al., 2008) were used as high and low values. The high EF was about 3.5 times the chosen EF, and the low value

was about half of the chosen EF. For changing the percentage of air exiting the CA/T exit as compared to Exit 26, percentages were shifted from 75% and 25% to 80% and 20% for a high percentage from the CA/T Exit, and 70% and 30% for a low percentage from the CA/T Exit. These percentages were incorporated into the emission rate calculations (Section 2.3). For varying the amount of cars, the number of cars for all sources was multiplied by 1.1 and 0.9 for high and low car values, respectively. Lastly, a calculated emission rate for VB #4 was used to compare with the CA/T operating certification. The emission rates for all sources for all model conditions are in Table 4.

Table 4. Calculated Emission Rates (g/s) for Sensitivity Analysis Scenarios in AERMOD.

	Emission Rate (g/s)			
Model Conditions	**CA/T Exit**	**Sumner Tunnel Exit**	**Exit 26**	**VB #4**
Baseline	0.100	0.027	0.006	0.208
High EF (EF = 0.189 g/veh/km)	0.365	0.097	0.023	0.208
Low EF (EF = 0.026 g/veh/km)	0.050	0.013	0.003	0.208
Percentage Exiting- 80%, 20%	0.107	0.027	0.005	0.208
Percentage Exiting- 70%, 30%	0.094	0.027	0.008	0.208
More Cars- Cars * 1.1	0.111	0.029	0.007	0.208
Fewer Cars- Cars * 0.9	0.090	0.024	0.006	0.208
VB #4 Calculation	0.101	0.027	0.006	0.022
TAPL EF (EF = 0.0079 g/veh/km)	0.015	0.004	0.001	0.208

2.7 Determination of Emission Factors from the CA/T Northbound Tunnel Bore

The same methodology from Perkins et al. (2012) was applied for using TAPL data to compute EFs. For simplicity, the traffic and TAPL data from Perkins et al. (2012) were used to understand if a computed EF fell into the same range as literature values. Two dates were analyzed for comparison with sensitivity analysis results: 1/6/2011 and 1/11/2011. For both dates, emission factors were determined by finding the linear regression line between mass of $PM_{2.5}$ per vehicle and distance through the tunnel (Figures A.5 and A.6). The computed emission factors from these two dates were averaged.

3.0 Results

3.1 Mobile Monitoring Data

Measured seasonal $PM_{2.5}$ concentrations in the CA/T are summarized in Table 5. As the TAPL moved through the CA/T, the $PM_{2.5}$ concentration increased as the cars pushed the polluted air through the tunnel bore, reaching a maximum close to the exit of the tunnel (Figure 3). The highest concentrations were measured in the summer with a median (± median average deviation) of 25.8 (±10.8) $\mu g/m^3$ (Table 5). The median concentrations in fall, winter, and spring were 21.0, 21.3, and 21.6 $\mu g/m^3$, respectively. These values were almost three times the median (7.9 ± 2.1 $\mu g/m^3$) of the North Street data, and were therefore sufficiently higher than background concentrations. Once the TAPL exits the tunnel, $PM_{2.5}$ concentrations rapidly decreased to background levels (Figure 3).

Table 5. Seasonal $PM_{2.5}$ Concentrations in the CA/T Measured using the TAPL.

	Northbound Tunnel				
Season	Fall	Winter	Spring	Summer	Total
# of trips	11	16	9	7	43
Median PM2.5 (MAD[1]) ($\mu g/m^3$)	21.0 (±10.2)	21.3 (±8.4)	21.6 (±6.0)	25.8 (±10.8)	21.6 (±7.8)
Range of PM2.5 ($\mu g/m^3$)	4.2 to 118.2	1.8 to 70.8	4.2 to 76.8	8.4 to 91.2	1.8 to 118.2

[1] MAD is the Median Average Deviation; MAD = median($| X_i - \text{median}(X) |$).

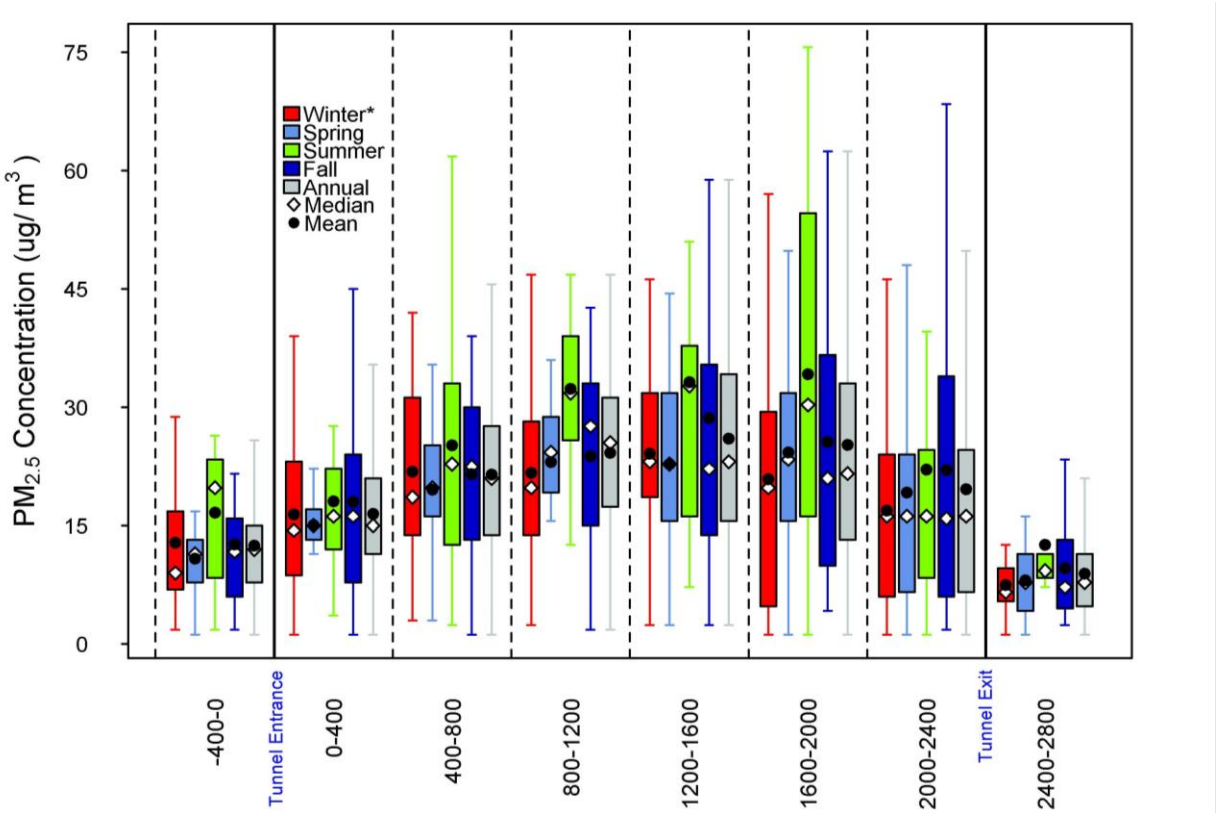

Figure 3. $PM_{2.5}$ Concentration in the Northbound I-93 Tunnel Collected between 12/14/2011 and 11/23/2013. Whiskers represent the smaller of the two values closest to Q3 + 1.5 * IQR and the larger of the two values closest to Q1 – 1.5 * IQR. *Fall = 9/23/11 to 12/21/11 and 9/22/12 to 12/20/12 and 9/22/13 to 12/20/13 (12 dates); Winter = 12/22/11 to 3/19/12 and 12/21/12 to 3/19/13 (13 dates); Spring = 3/20/12 to 6/19/12 and 3/20/13 to 6/20/13 (9 dates); Summer = 6/20/12 to 9/21/12 and 6/21/13 to 9/21/13 (7 dates).

3.2 EPA Stationary Site $PM_{2.5}$ Data Comparison

3.2.1 Annual $PM_{2.5}$ Trends

Average $PM_{2.5}$ concentrations decreased over the five years at all three sites (Figures 4–6). The highest $PM_{2.5}$ concentration measured over the five years at the North Street site was 38.7 µg/m^3 in January 2011, and all values were below 25.0 µg/m^3 after January 2011. Between 2011 and 2015, $PM_{2.5}$ concentrations at the North Street site decreased on average by 0.77 µg/m^3/year (Figure 4). In comparison, the rate of decrease over time at the Blue Hill Observatory site was 0.073 µg/m^3/year (Figure 5). The $PM_{2.5}$ concentrations at the Blue Hill Observatory was

generally lower than those at the North End, and the annual decrease in $PM_{2.5}$ was nearly ten times less than at the North Street site. The rate of decrease at the Lynn site was 0.475 $\mu g/m^3$/year (Figure 6).

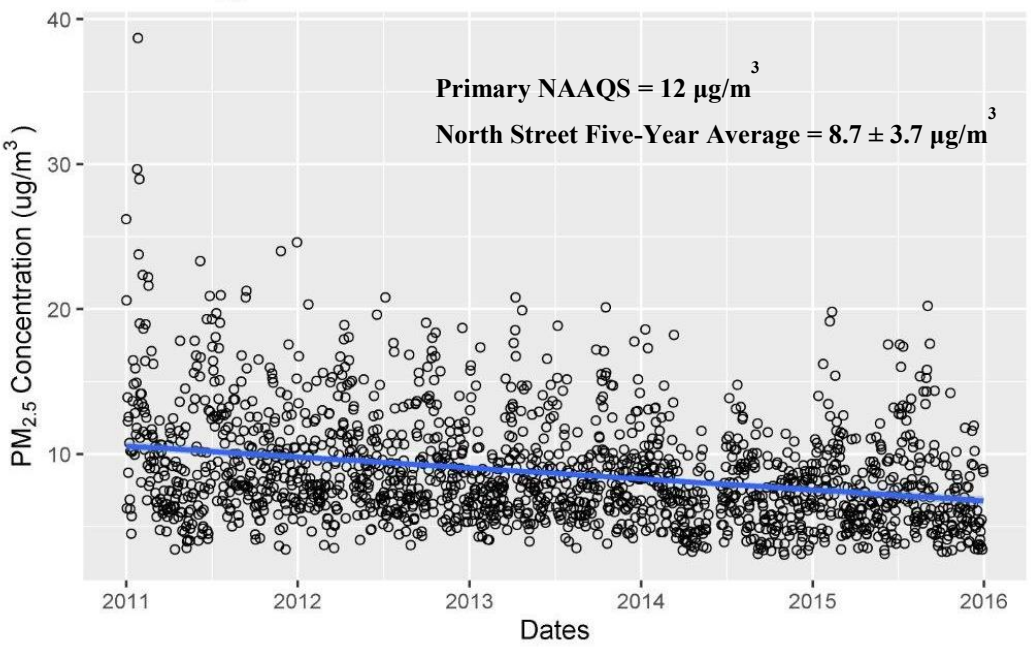

Figure 4. $PM_{2.5}$ FRM Concentration at North Street (#25-025-0043) for 2011–2015 (slope = -0.767 $\mu g/m^3$/year, $r^2 = 0.0857$).

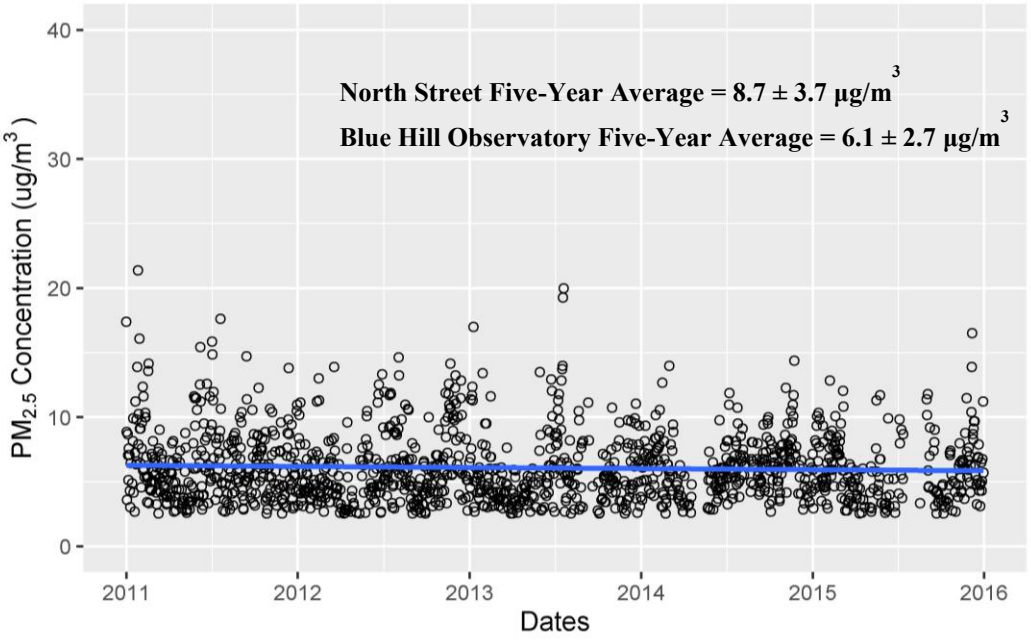

Figure 5. $PM_{2.5}$ Adjusted Concentration at the Blue Hill Observatory (#25-021-3003) for 2011–2015 (slope = -0.073 $\mu g/m^3$/year, $r^2 = 0.002$).

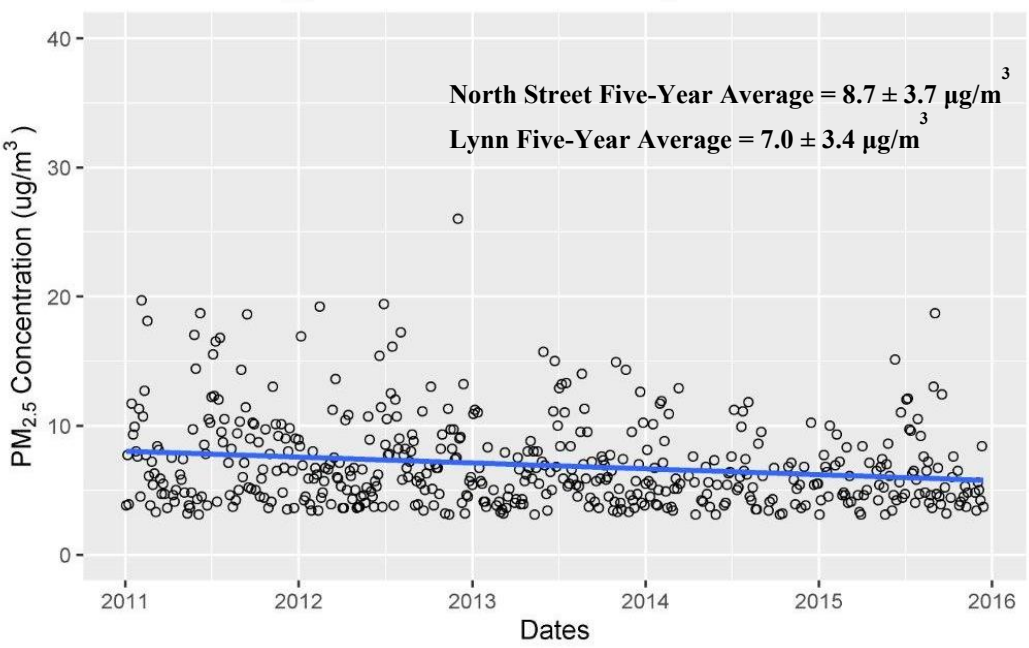

Figure 6. $PM_{2.5}$ FRM Concentration at Lynn (#25-009-2006) for 2011–2015 (slope = -0.475 µg/m^3/year, $r^2 = 0.0356$).

3.2.2 Seasonal $PM_{2.5}$ Trends

There was not much seasonal variation within sites (Figures 7, A.7, A.8). For the North Street and the Blue Hill Observatory sites, the highest seasonal median $PM_{2.5}$ concentrations were observed in the winter, followed by the summer, fall, and spring (Table 6). In Lynn, the greatest seasonal median was observed during the summer, followed by the winter, fall, and spring. However, these differences were not significant.

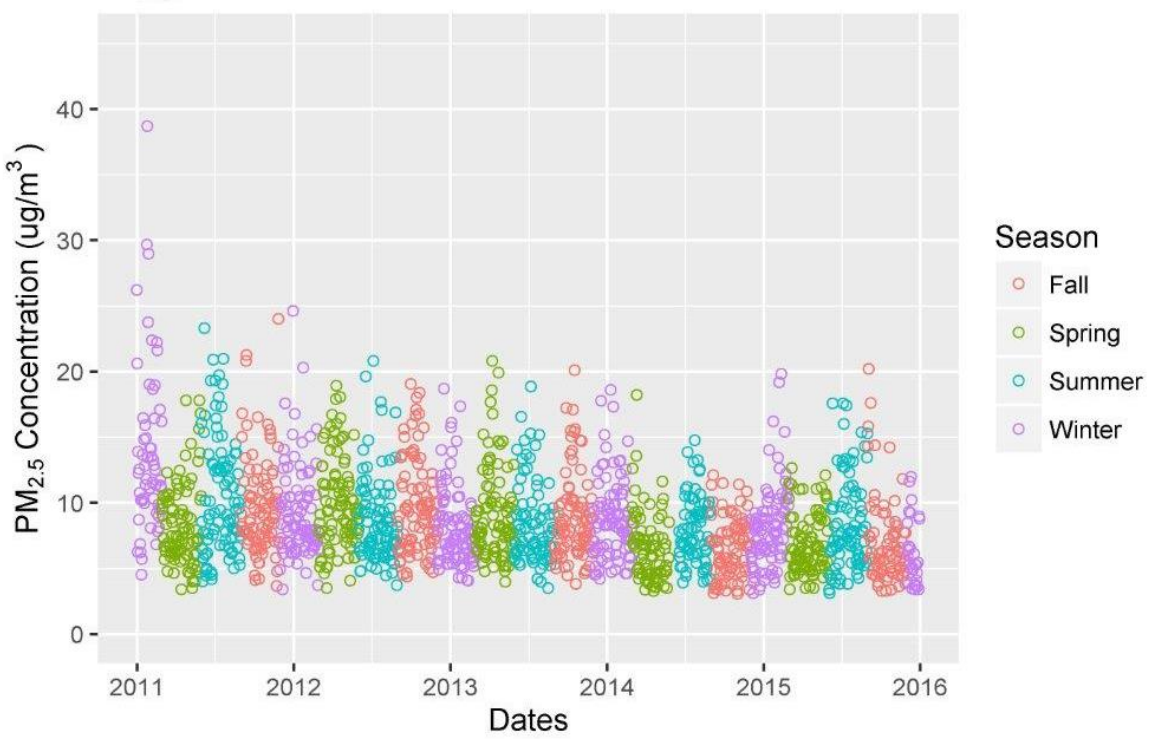

Figure 7. $PM_{2.5}$ FRM Concentration at North Street (#25-025-0043) by Season for 2011–2015. Seasons: Winter (December, January, February), Spring (March, April, May), Summer (June, July, August), Fall (September, October, November).

Table 6. Seasonal Median $PM_{2.5}$ Concentrations ($\mu g/m^3$) for each Dataset for 2011–2015 and the Adjusted Blue Hill Observatory Data. Winter = December, January, February; Spring = March, April, May; Summer = June, July, August; Fall = September, October, November.

Site	Method	Winter Median (MAD)	Winter Count	Spring Median (MAD)	Spring Count	Summer Median (MAD)	Summer Count	Fall Median (MAD)	Fall Count	Annual Median (MAD)	Total Count
Blue Hill Observatory (25-021-3003)	FEM	7.3 (2.0)	400	5.6 (1.5)	306	7.25 (2.1)	344	7.05 (1.95)	354	6.8 (1.9)	1404
Blue Hill Observatory (25-021-3003	Adjusted	5.9 (1.6)	400	4.5 (1.2)	306	5.9 (1.7)	344	5.7 (1.6)	354	5.5 (1.5)	1404
Lynn (25-009-2006)	FRM	5.95 (1.95)	122	5.5 (1.45)	120	7.05 (2.45)	136	5.8 (1.7)	115	6.0 (1.8)	493
North End (25-025-0043)	FRM	8.275 (2.075)	446	7.5 (2.0)	442	8.0 (2.0)	423	7.8 (2.0)	421	7.9 (2.05)	1732

There was not much seasonal variation when $PM_{2.5}$ concentration at each site was varied by wind direction (Figures 8, A.9, A.10).

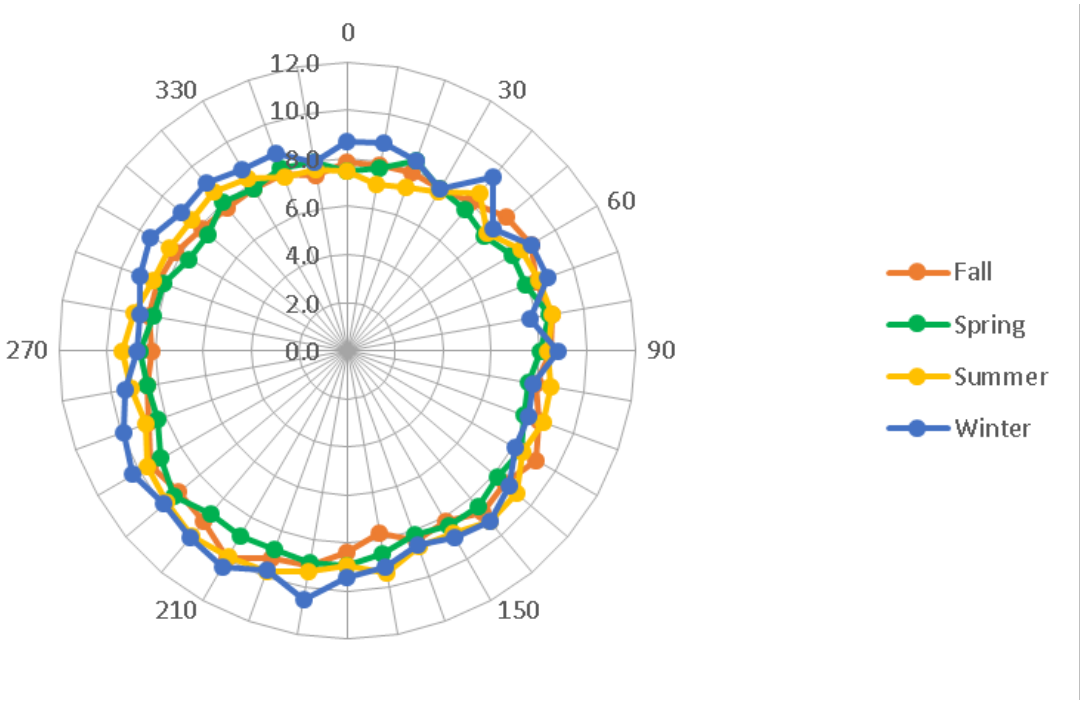

Figure 8. Seasonal $PM_{2.5}$ FRM Concentration Rose of Ten-Degree Averaged Wind Bins at North Street (#25-025-0043) for 2011–2015. Seasons: Winter (December, January, February), Spring (March, April, May), Summer (June, July, August), Fall (September, October, November).

3.2.3 Wind-Direction and Difference $PM_{2.5}$ Trends

$PM_{2.5}$ concentrations at the three sites were greatest when winds were from the southwest (Figure 9). This could be from a higher amount of sulfur-related particulate matter. Sulfates can be used to measure regional pollution, which could come from cities along the East Coast, such as New York City and Philadelphia.

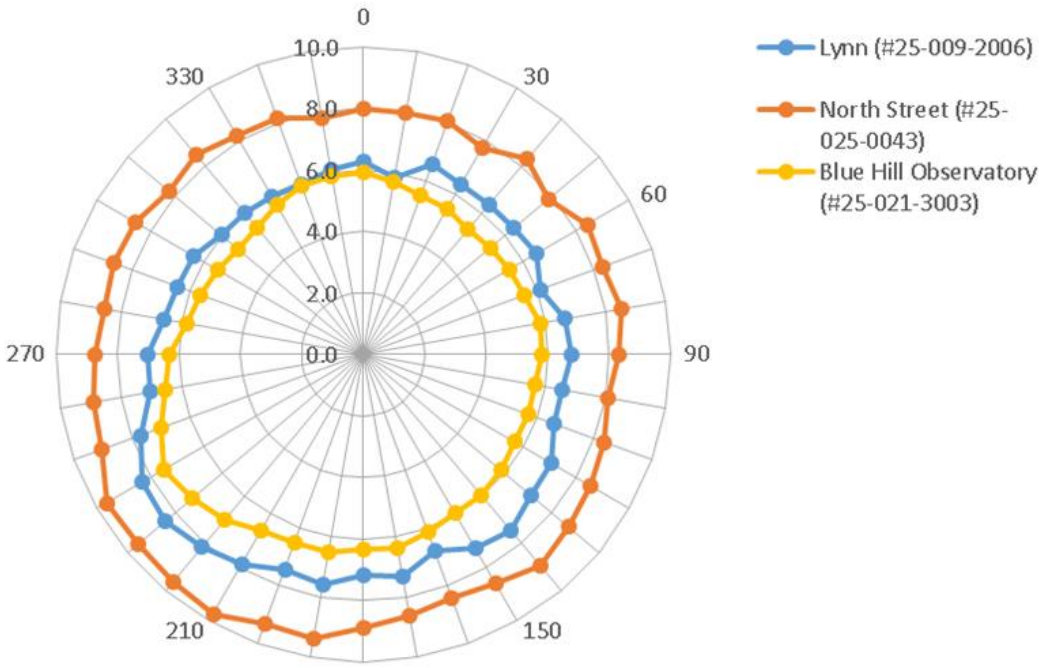

Figure 9. $PM_{2.5}$ Concentration Rose of Ten-Degree Averaged Wind Bins for the three EPA sites for 2011–2015.

Differences between North Street and the Blue Hill Observatory by wind direction ranged from 2.0 to 3.6 µg/m^3 by ten-degree wind sector (Figure 10). The greatest differences between $PM_{2.5}$ concentrations at North Street and the Blue Hill Observatory were when winds came from the northwest, northeast, and southwest. The overall median difference between all North Street and Blue Hill Observatory data was 2.8 µg/m^3 (1335 dates). Differences between North Street and Lynn by wind direction ranged from 1.2 to 3.4 µg/m^3 by ten-degree wind sector (Figure 11). The differences between North Street and Lynn $PM_{2.5}$ concentrations were greatest when winds came from the northwest. The overall median difference between all North Street and Lynn data was 2.4 µg/m^3 (481 dates). Since the median $PM_{2.5}$ concentration at North Street is 7.9 µg/m^3, local $PM_{2.5}$ sources contribute between 30 and 35% of the total $PM_{2.5}$.

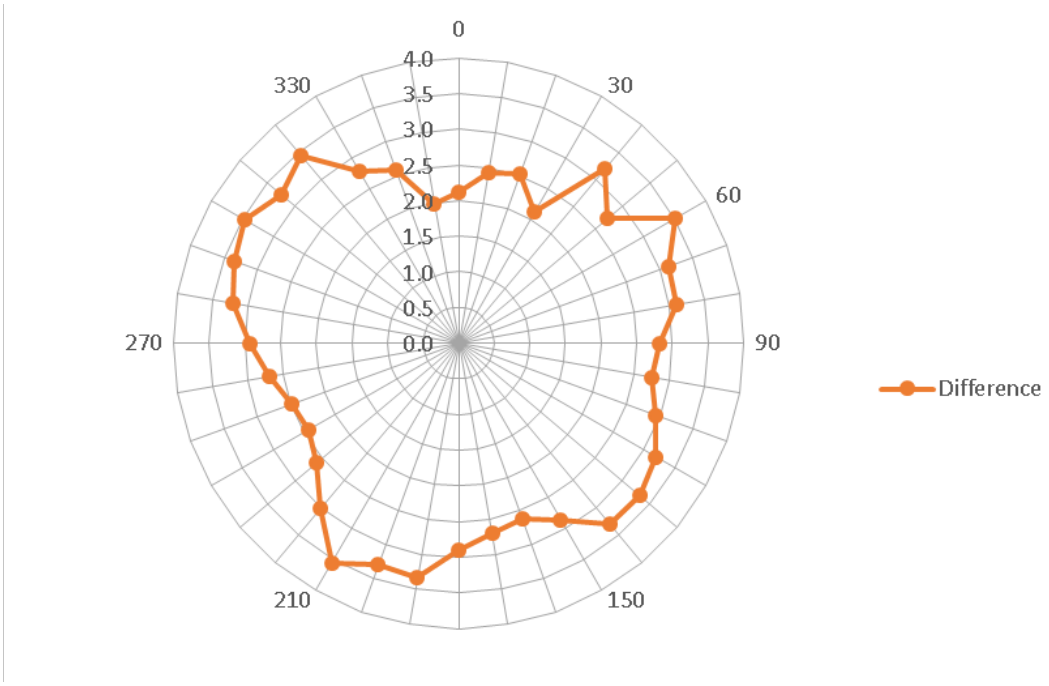

Figure 10. $PM_{2.5}$ Concentration Difference Rose of Ten-Degree Averaged Wind Bins between North Street and the Blue Hill Observatory for 2011–2015.

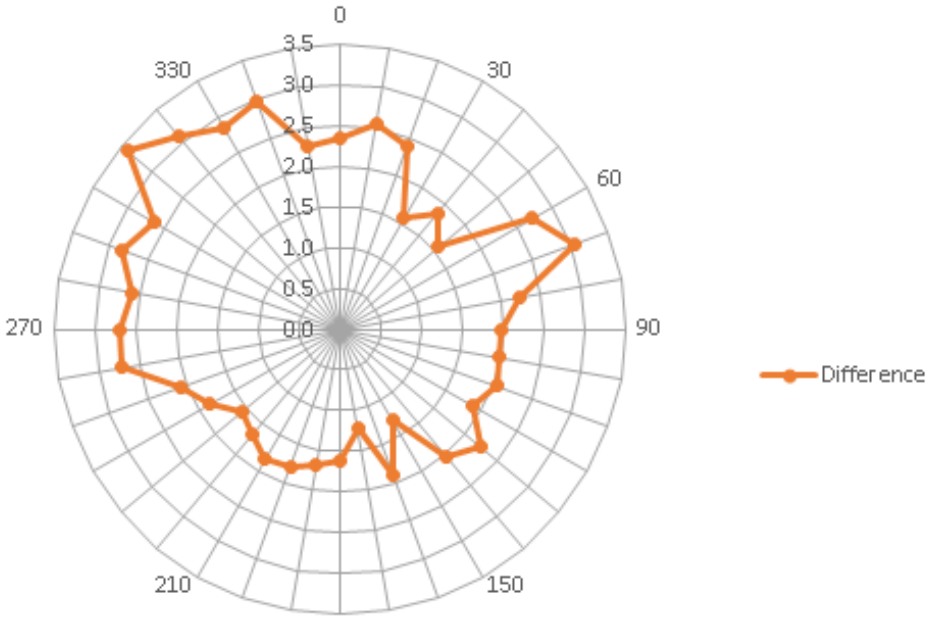

Figure 11. $PM_{2.5}$ Concentration Difference Rose of Ten-Degree Averaged Wind Bins between North Street and Lynn for 2011–2015.

3.2.4 Weekly $PM_{2.5}$ Trends

When weekends (Saturday and Sunday) were compared to weekdays (Monday through Friday), $PM_{2.5}$ concentrations at North Street did not vary much (Figure 12). Similar results were found at the Blue Hill Observatory and Lynn (Figures A.11 and A.12). Therefore, differences between weekend and weekday $PM_{2.5}$ concentrations trends were not substantial.

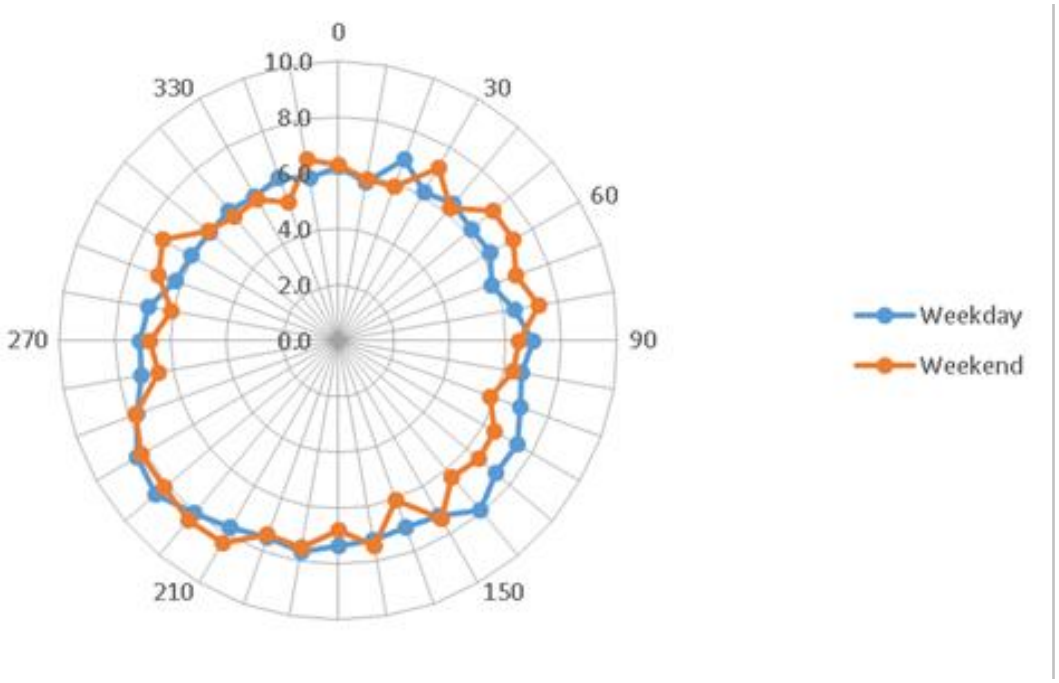

Figure 12. Weekend and Weekday FRM $PM_{2.5}$ Concentration Rose of Ten-Degree Averaged Wind Bins at North Street (#25-025-0043) for 2011–2015. Classifications: Weekends (Saturday, Sunday), Weekdays (Monday, Tuesday, Wednesday, Thursday, Friday).

3.3 AERMOD $PM_{2.5}$ Modeling

3.3.1 Southwest Winds (240°) (Mimics Summer) Scenario

Modeled and measured results were compared for twelve time periods of at least three days each with 20%, 30%, and 40% of hourly wind direction measurements within 20°, 30°, and 40° of 240° from due north (Table 3). Measured values were considered to be the difference between $PM_{2.5}$ concentrations measured at North Street and the adjusted value at the Blue Hill Observatory. The model has a much smaller range of values than the differences between the two

sites (Figure 13). The differences ranged from -11.6 to 14.5 µg/m^3, whereas modeled data ranged from 0.4 to 3.2 µg/m^3. Differences were negative in some cases when the adjusted $PM_{2.5}$ concentrations at the Blue Hill Observatory were greater than the $PM_{2.5}$ concentrations at North Street. The overall average for the differences was 0.4 µg/m^3, compared to 1.5 µg/m^3 for the modeled data (Table 7). Since many more factors influenced measured $PM_{2.5}$ concentrations than what the modal accounted for, variation was much greater in the differences between the two sites.

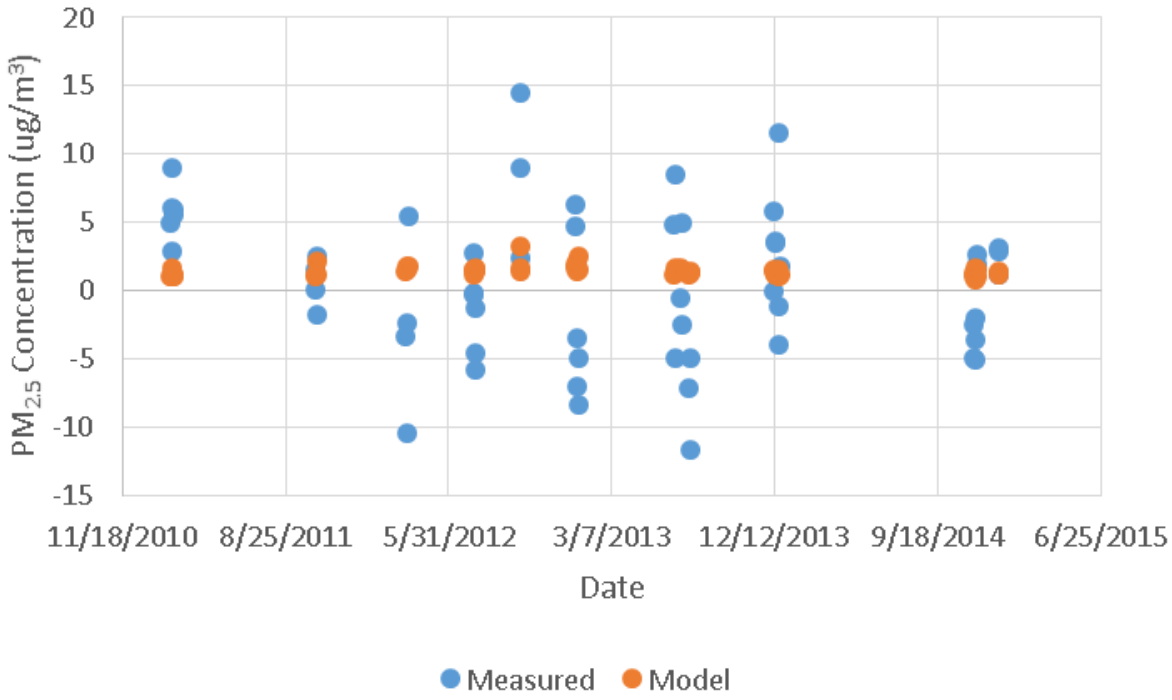

Figure 13. The Comparison of Measured and Modeled $PM_{2.5}$ Data for Southwest (240º) Winds. Measured = $PM_{2.5}$(North Street) – $PM_{2.5,adj.}$(Blue Hill Observatory).

Table 7. Southwest Winds (Mimics Summer) Scenario Results by Time Period for 2011–2015.

Time Period	# Days	Measured Avg. (μg/m^3)	Model Avg. (μg/m^3)
2/9/2011-2/14/2011	6	5.7	1.3
10/15/2011-10/18/2011	4	0.6	1.4
3/18/2012-3/20/2012	3	-5.3	1.6
7/12/2012-7/17/2012	6	-1.5	1.5
9/30/2012-10/2/2012	3	8.6	2.1
1/4/2013-1/9/2013	6	-2.1	1.9
6/22/2013-6/24/2013	3	1.7	1.7
7/4/2013-7/6/2013	3	0.7	1.5
7/18/2013-7/20/2013	3	-7.8	1.3
12/10/2013-12/13/2013	4	3.3	1.4
11/19/2014-11/25/2013	7	-1.9	1.3
12/31/2014-1/2/2015	3	2.4	1.3
Average	51	0.4	1.5

3.3.2 Northwest Winds (300°) (Mimics Winter) Scenario

Modeled and measured results were compared for nine time periods of at least three days each with 20%, 30%, and 40% of hourly wind direction measurements within 20°, 30°, and 40° of 300° from due north (Table 3). Measured values were considered to be the difference between $PM_{2.5}$ concentrations measured at North Street and the adjusted value at the Blue Hill Observatory. Since winds in Boston come from the west and northwest more frequently during winter months (Figure A.4), six out of the nine time periods were between January and March (in this analysis, "spring" months are March, April, and May). The differences ranged from -3.6 to 13.0 μg/m^3, whereas modeled data ranged from 0.4 to 2.5 μg/m^3 (Figure 14). The overall average for the differences was 3.4 μg/m^3, compared to 1.1 μg/m^3 for modeled data (Table 8).

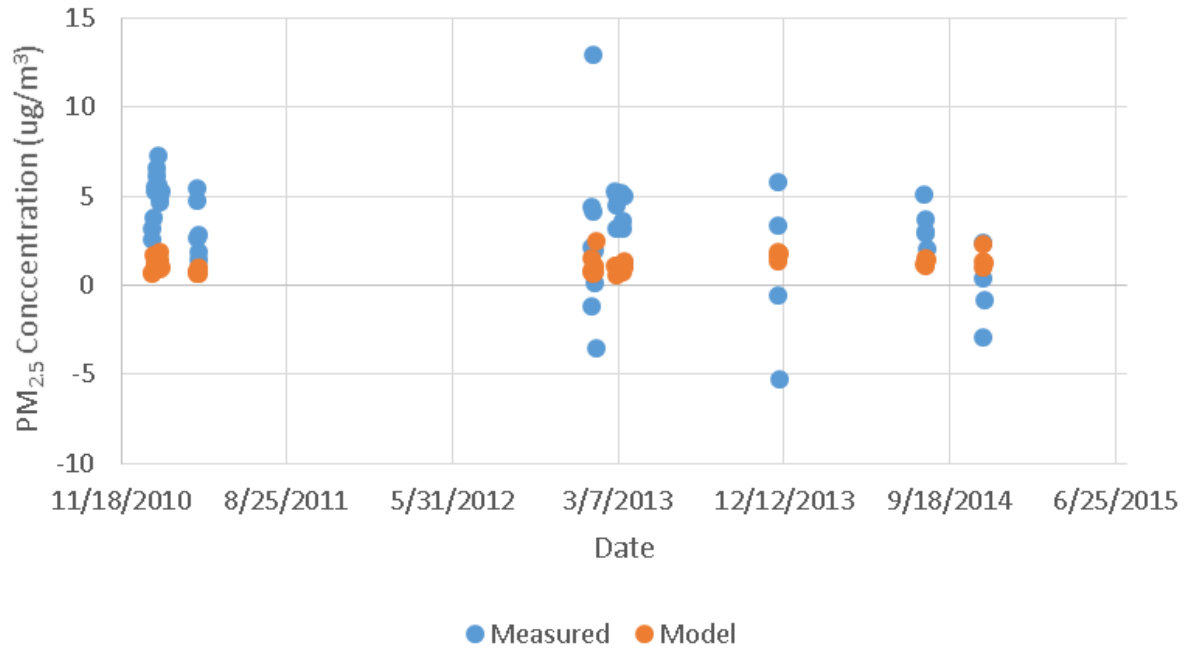

Figure 14. The Comparison Measured and Modeled $PM_{2.5}$ Data for Northwest (300º) Winds. Measured = $PM_{2.5}$(North Street) – $PM_{2.5,adj.}$(Blue Hill Observatory).

Table 8. Northwest Winds (Mimics Winter) Scenario Results by Time Period for 2011–2015.

Time Period	# Days	Measured Avg. (µg/m^3)	Model Avg. (µg/m^3)
1/9/2011-1/11/2011	3	3.2	1.0
1/14/2011-1/24/2011	10*	5.6	1.3
3/25/2011-3/30/2011	6	3.2	0.8
1/20/2013-1/28/2013	9	2.4	1.1
3/2/2013-3/5/2013	4	4.5	1.0
3/13/2013-3/17/2013	5	3.6	1.0
8/6/2014-8/10/2014	5	3.4	1.3
11/12/2014-11/15/2014	4	-0.3	1.5
Average	46	3.4	1.1

3.3.3 The Proximity of the Tunnel Exits

Model results were compared for the four sources, all sources but the Sumner Tunnel Exit, and all sources but the CA/T exit (Table 9). The differences between the averages for the four sources and the averages for all sources but the Sumner Tunnel Exit for the southwest and northwest wind scenarios were 0.85 and 0.91 µg/m^3, respectively. The differences between the

averages for the four sources and the averages for all sources but the CA/T Exit for the southwest and northwest wind scenarios were 0.03 and 0.05 μg/m^3, respectively. These results showed that proximity affects the impact of the source. Although the emission rate for the CA/T Exit was about four times greater than the emission rate for the Sumner Tunnel Exit because of differences in traffic volume, the Sumner Tunnel Exit contributed substantially more $PM_{2.5}$ to the North Street site because it was 60 meters in distance, compared to the CA/T Exit, which was about 640 meters from the North Street site.

Table 9. $PM_{2.5}$ AERMOD Average Results for Two Scenarios under Three Different Modeling Conditions for 2011–2015. SD = Standard Deviation.

			Model Avg. (SD) (μg/m^3)		
Scenario	# Days	Measured Avg. (SD) (μg/m^3)	Four Sources	No Sumner Exit	No CA/T Exit
Southwest Winds (Mimics Summer)	51	0.38 (5.37)	1.49 (0.41)	0.64 (0.24)	1.46 (0.40)
Northwest Winds (Mimics Winter)	46	3.45 (2.77)	1.12 (0.41)	0.21 (0.11)	1.07 (0.39)

3.3.4 Sensitivity Analysis

Changing the EF had the greatest impact on the results. The EF had a linear relationship with the average model $PM_{2.5}$ concentration (Figure 15). When the highest EF evaluated (0.189 g/veh/km) was used for the 2/9/2011–2/14/2011 and 1/14/2011–1/24/2011, the average $PM_{2.5}$ model results at the North Street receptor were 2.95 and 4.28 grams per vehicle per kilometer, respectively (Table 10). This is a factor of about 2.4 and 3.4 times greater compared to the baseline model conditions. When the low EF of 0.026 grams per vehicle per kilometer was used, the average values for southwest and northwest winds were 0.89 and 0.66 μg/m^3, respectively. The high and low EFs had a greater impact on the northwest winds scenario, as compared to the southwest winds scenario. Changing the percentage of air exiting the CA/T Exit and Exit 26 had very little effect on either scenario. Varying the amount of cars had a minimal effect on both

scenarios. Using the calculated emission rate for VB #4 had very little effect on the northwest wind scenario, but a more sufficient impact on the southwest wind scenario. This may have been because VB #4 was southwest of the North Street receptor.

Table 10. $PM_{2.5}$ AERMOD Average Results for Two Time Periods for Different Modeling Scenarios and Emission Factors.

	Time Period	2/9/2011-2/14/2011	1/14/2011-1/24/2011
	Scenario	SW Winds	NW Winds
	# Days	6	10
	Measured Avg. ($\mu g/m^3$)	5.74	5.64
Model Average ($\mu g/m^3$)	Baseline	1.25	1.26
	No CA/T Exit	1.23	1.20
	No Sumner Exit	0.55	0.23
	High EF (EF = 0.189 g/veh/km)	2.95	4.28
	Low EF (EF = 0.026 g/veh/km)	0.89	0.67
	VB #4 Calculation	0.78	1.11
	TAPL EF (EF = 0.0079 g/veh/km)	0.64	0.34
	Percentage Exiting- 80%, 20%	1.25	1.17
	Percentage Exiting- 70%, 30%	1.25	1.26
	More Cars- Cars * 1.1	1.33	1.37
	Less Cars- Cars * 0.9	1.18	1.15

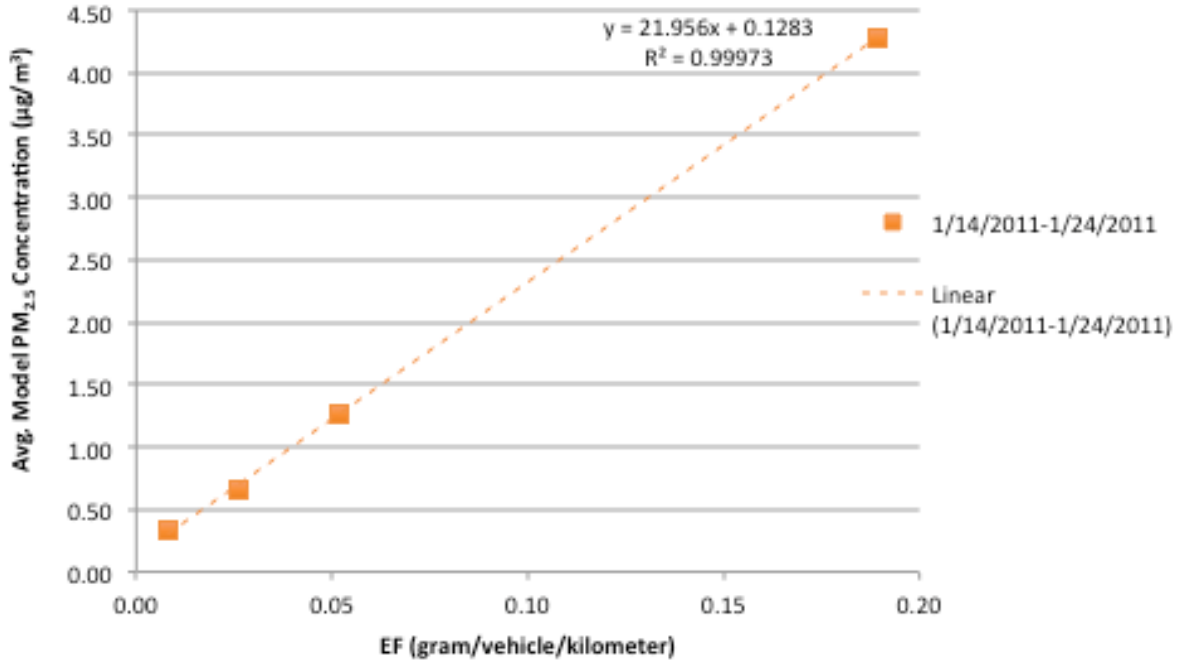

Figure 15. The Average $PM_{2.5}$ Concentration compared to the Emission Factor (grams per vehicle per kilometer) used in AERMOD for 1/14/2011–1/24/2011 (excluding 1/18/2011) (slope = 21.956, r^2 = 0.99973).

3.3.5 Model Performance Evaluation

To evaluate the model results, a factor-of-two percentage envelope was used to see if the $PM_{2.5}$ measured differences were between half of the modeled data and two times the modeled data (Milando, 2012; Yura et al., 2007). The model produced poor results according to this approach. In the southwest winds scenario (240°), 5 out of 51 days (61.5%) of the analyzed days fell within this envelope. In the northwest winds scenario (300°), 7 out of 46 days (15.2%) analyzed fell within this factor of two. However, this assumes that 100% of the difference between the measured value at North Street and the Blue Hill Observatory may be attributed to mobile, tunnel-related sources.

Adjustment factors for each scenario were determined by maximizing the number of dates that fell within the factor-of-two envelope. The optimal adjustment factor for the southwest winds scenario was between 0.33 and 0.42. This range had 20 out of 51 values fall within the factor-of-two envelope (39.2%). This value was low because 24 out of the 51 values in this scenario had negative measured values, meaning that $PM_{2.5}$ concentrations at the Blue Hill Observatory were greater than $PM_{2.5}$ concentrations at the North Street site on that day. The optimal adjustment factor for the northwest winds scenario was 0.29 to 0.30. This range had 33 out of 46 values (71.7%) fall within the factor-of-two envelope.

3.4 Emission Factor Results from the CA/T Northbound Tunnel Bore

On 1/6/2011 and 1/11/2011, the computed EFs were 0.0064 and 0.0094 grams per vehicle per kilometer, respectively. This averaged to an EF of 0.0079 grams per vehicle per kilometer. This was about 6.5 times less than the literature value used from Gillies et al. (2001). This was about 3 times lower than the lowest literature value found (Handler et al., 2008) and 33 times lower

than the greatest value found (Cheng et al., 2006). The emission rates using this EF for the four sources are in Table 3. The average model results for the two time periods (2/9/2011–2/14/2011 and 1/14/2011–1/24/2011) used in the sensitivity analysis were 0.64 and 0.34 $\mu g/m^3$, respectively.

4.0 Discussion

4.1 The Contribution of Mobile Sources to $PM_{2.5}$ Concentrations in Boston, MA

Urban $PM_{2.5}$ sources contribute about one-third of total $PM_{2.5}$ concentrations in Boston, MA (Section 3.2.3). From AERMOD, mobile sources may contribute between 14% and 19% of the total ambient $PM_{2.5}$ measured at North Street (Sections 3.3.1 and 3.3.2); however this does not take into account the impacts of the emission factor used, nor does it take into account differing patterns between measured and modeled data. This range falls within that measured in the literature. In a monitoring study in Treviso, Italy, $PM_{2.5}$ contributions from road transport in two municipalities were determined to be 12.3% and 22.5%. The contribution from road transport at the provincial level was 20.9% (Squizzato et al., 2017). This is around the same range that AERMOD predicted for Boston. In a monitoring study in five cities in Connecticut and Massachusetts in the early 2000s, motor vehicles and road dust contributed between 33% and 46% of ambient $PM_{2.5}$ concentrations (Lee et al., 2011a). If road dust was not included, motor vehicles contributed between 25% and 31% to ambient $PM_{2.5}$ concentrations. This range may be greater than that seen in this work because of limitations in the sources accounted for in the model or because of greater emissions in older vehicles.

A recent modeling effort in New York City used CMAQ at a 1-kilometer resolution to understand $PM_{2.5}$ contributions from traffic. This study found that traffic contributed 0.38 to 2.60 $\mu g/m^3$ (3.9% to 22.7%) throughout 1-kilometer grid cells within New York City (Kheirbek et al., 2016). In comparison, two earlier studies estimated that $PM_{2.5}$ source contribution from mobile sources ranges from 16% to 39% of total ambient $PM_{2.5}$ concentrations (Ito et al., 2004; Lall & Thurston, 2006). The results from the modeling study were lower than the earlier studies, possibly because of limitations in the locations and number of monitors on the source-apportionment studies or because of updated traffic emissions estimates resulting in lower emissions (Kheirbek et al., 2016). Similar limitations in this work may have resulted in lower percentages of modeled $PM_{2.5}$ contributions to ambient $PM_{2.5}$ concentrations.

A study that looked at contributions in different regions of the U.S., found that $PM_{2.5}$ attributable to mobile sources ranged from 0.4 to upwards of 6 $\mu g/m^3$ (Engel-Cox & Weber, 2007). Therefore, there is a wide range for the amount of $PM_{2.5}$ contributed by mobile sources to ambient $PM_{2.5}$ levels. However, the results from this work fall within the range in the literature.

4.2 The Impact of Proximity on $PM_{2.5}$ Contributions

As shown in the comparison of the impacts of the Sumner Tunnel Exit and the CA/T Exit on AERMOD results at the North Street receptor, proximity to the source has a sufficient impact. Although the Sumner Tunnel Exit had about one fourth the amount of traffic that the CA/T Exit had, the Sumner Tunnel Exit had a greater impact on the $PM_{2.5}$ model results at North Street. This is because the Sumner Tunnel Exit was about 60 meters from the North Street receptor, as opposed to the CA/T Exit, which was about 640 meters in distance (Figure 1). The Sumner Tunnel Exit still had a small overall effect on $PM_{2.5}$ concentrations at North Street compared to

overall ambient levels. This result aligns with other studies' conclusions on the contribution of local $PM_{2.5}$ concentrations near roadways to ambient $PM_{2.5}$ concentrations (Ginzburg et al., 2015; Padró-Martínez et al., 2012).

4.3 Validity and Impacts of Assumptions

4.3.1 Determination of Emission Factors

The EF used (0.052 grams per vehicle per kilometer) was developed for the Sepulveda Tunnel in Los Angeles, California (Gillies et al., 2001). Although Los Angeles has a very different climate than Boston, the Sepulveda Tunnel has similar proportions of diesel vehicles as the CA/T, which greatly impacts $PM_{2.5}$ emissions. Additionally, this EF was more conservative than many others found in the literature (Table 2). One shortcoming of this EF is that it is an annual value, and is not differentiated by season, vehicle speed, amount of traffic, or any additional factors. Although the model results are daily averaged values, these values could be more accurate if the EF in the model took into account various factors that impact the amount of vehicles and the amount of $PM_{2.5}$ emitted from a vehicle at any given time. As the data and literature have shown, season and temperature impact the composition and quantity of $PM_{2.5}$ (Bell et al., 2007; Lee et al., 2011a; Padró-Martínez et al., 2012; Patton et al., 2014). Additionally, vehicle speed impacts the EF and the number of vehicles impacts the emission rate, which is calculated using the EF (Grieshop et al., 2006). The sensitivity analysis showed that the EF had a linear relationship with the modeled $PM_{2.5}$ concentration (Figure 15). Therefore, choice of EF has a major impact on the $PM_{2.5}$ modeled concentrations.

4.3.2 Daily Pollutant Data to Hourly Meteorological Data

Another assumption made in this analysis was that averaged daily $PM_{2.5}$ concentrations could be merged with hourly wind speed and direction data. Daily averaged $PM_{2.5}$ concentrations were the finest resolution of data available from the EPA monitors; however, most likely, the $PM_{2.5}$ concentration varied throughout the day. By merging hourly wind speed and direction data with daily $PM_{2.5}$ data, it was assumed that the daily concentration value reflects that for all wind directions over the course of a 24-hour day and for all temperature, meteorological, and traffic variances over the course of a day.

4.3.3 Proportion of Pollution Exiting Exit 26 versus the CA/T Exit

In calculating the emission rates for the CA/T main exit and Exit 26, it was assumed that 25% of the air traveling through the tunnel exited through Exit 26 and the other 75% of the air traveling through the tunnel exited at the main exit. When this was varied through the sensitivity analysis, no change was detected for the southwest winds scenario, and negligible change was detected for the northwest winds scenario. Therefore, the proportion of pollution going through Exit 26 and the CA/T Exit did not impact model results.

4.3.4 Tunnel Exits as Volume or Point Sources

Model results were compared analyzing the tunnel exits as volume and point sources. The main difference between the two is that a volume source is a three-dimensional plume, whereas a point source is one-dimensional. The values for both source types were very similar, and so this parameter had a negligible impact on model results. It was chosen to model the exits as volume sources because other work has done the same (Ginzburg & Schattanek, 1997) and because this approach seemed more realistic in how air moves away from a tunnel exit.

4.3.5 Building Downwash

Building downwash accounts for the effects of turbulent wake zones around buildings that may force air to rise (Missouri Department of Natural Resources, 2013). The EPA developed a preprocessing tool to take building downwash into account; this tool is called the Building Profile Input Program with Plume Rise Model Enhancements. For simplicity, this model does not take building downwash into account. Most likely, building downwash in AERMOD would not have a large impact on results because building downwash effects are only considered for point sources (Missouri Department of Natural Resources, 2013). Since three out of the four model sources are volume sources, incorporating building downwash would not affect these sources. However, since the North Street area is very urban, and air exiting the CA/T and the Sumner Tunnel is at street level, nearby buildings do impact wind turbulence and movement.

4.3.6 Time Periods Modeled

For the southwest and northwest wind scenarios, time periods were chosen based on having at least three days with 20%, 30%, and 40% of hourly wind direction measurements within 20°, 30°, and 40° of the specified direction (240° or 300°) from due north. The goal through these exclusion criteria was to find time periods that were long enough for wind direction to impact daily $PM_{2.5}$ concentrations, and with enough wind in the given direction for sources from that direction to be detectable. However, these criteria were arbitrarily chosen, and increasing or decreasing the length of time and the percentage of hourly wind data could impact the comparison of modeled and measured data.

4.4 Future Work

4.4.1 Central Artery/Tunnel Exit Monitoring Campaign

Past studies suggest that a large proportion of ambient $PM_{2.5}$ concentrations can be attributed to regional sources, and that as distance from highways and roads increases, $PM_{2.5}$ concentrations stay about level. Rather, $PM_{2.5}$ concentration is impacted by temperature and wind direction. (Bell et al., 2007; Padró-Martínez et al., 2012; Patton et al., 2014) Measured and modeled results analyzed in this project also suggest this. In order to improve further modeling, future $PM_{2.5}$ monitoring could be done. According to the model results, especially from comparisons with and without the Sumner Tunnel, $PM_{2.5}$ concentrations may be elevated by just under 1.0 $\mu g/m^3$ within the vicinity of the Sumner Tunnel Exit. Since the CA/T northbound exit is about 640 meters from the EPA North Street site, adding an instrument or two immediately within the vicinity of the CA/T exit could result in more accurate data to compare to AERMOD.

One recommendation is to add $PM_{2.5}$ monitors about 10 meters and 400 meters north of the CA/T Northbound exit. Since vehicles from the tunnel are pushing air north out of the tunnel, theoretically, elevated $PM_{2.5}$ concentrations could be measured at the monitor close to the exit. When these two distances were added as ground-level receptors in AERMOD, the maximum $PM_{2.5}$ source contributions at the 10-meter and 400-meter receptors between 2011 and 2015 were 183 and 0.7 $\mu g/m^3$, respectively. The average $PM_{2.5}$ concentrations over the five-year period were 67 and 0.1 $\mu g/m^3$. Therefore, 10 meters is a good location to measure maximum $PM_{2.5}$ concentrations, and 400 meters is far enough to measure background $PM_{2.5}$ levels.

Another recommendation is to add a $PM_{2.5}$ monitor above the CA/T Exit. This could measure and account for $PM_{2.5}$ that immediately rises upon exiting the tunnel as a result of being warmer than ambient air. Additionally, TAPL data showed that $PM_{2.5}$ levels along the road

decreased rapidly upon exiting the tunnel, providing the possibility that plumes of $PM_{2.5}$ rise upon exiting the tunnel, rather than moving further away from the tunnel.

4.4.2 Central Artery/Tunnel Commuter Exposure Work

Another direction for future work is an expansion of monitoring inside the CA/T tunnel bores. Since measured $PM_{2.5}$ levels within the tunnel are significantly higher than background $PM_{2.5}$ levels, more work could be done to understand exposure levels for commuters traveling within the tunnel. This could be done through more measurements using the TAPL, as well as taking measurements when the windows are up and down to determine the concentration of $PM_{2.5}$ entering the cabins of vehicles. In Cains et al. (2003), average $PM_{2.5}$ concentrations measured in the M5 East Tunnel in Sydney, Australia were about six times as high when the windows were down. Additionally, more information on vehicle speeds, traffic congestion levels, and time of vehicles inside the tunnel would be beneficial to better understand exposure.

5.0 Conclusions

Overall, the measurement campaigns analyzed show that $PM_{2.5}$ levels in the Boston metropolitan area are below the NAAQS. However, elevated $PM_{2.5}$ concentrations have been measured within the CA/T; these elevated levels impacted localized areas within close proximity to the CA/T. $PM_{2.5}$ concentrations in the entire region were highest when winds came from the southwest, providing evidence for the regional contribution of $PM_{2.5}$. Modeled results showed the local influence of $PM_{2.5}$ concentrations from mobile tunnel-related sources; although the local mobile component of $PM_{2.5}$ was small compared to regional sources, it still impacted overall $PM_{2.5}$ levels in Boston. In order to better understand $PM_{2.5}$ levels in the immediate vicinity of the CA/T

exits, measurement campaigns closer to the exits should be implemented. Future work may also focus on exposure levels for commuters traveling within the CA/T.

6.0 Acknowledgements

Thank you very much to Professor John Durant, Dr. Allison Patton, Matt Simon, Dr. Neelakshi Hudda, and Jess Perkins for guidance, ideas, and support throughout this project. Thank you very much to the CAFEH study and Professor John Durant's lab for giving me access to the TAPL dataset.

7.0 References

Balczo, M., Balogh, M., Goricsan, I., Nagel, T., Suda, J. M., & Lajos, T. (2011). Air quality around motorway tunnels in complex terrain - computational fluid dynamics modeling and comparison to wind tunnel data. *Idojaras*, *115*(3), 179–204.

Bates, D. V. (1992). Health indices of the adverse effects of air pollution: the question of coherence. *Environmental Research*, *59*(2), 336–349.

Bell, M. L., Dominici, F., Ebisu, K., Zeger, S. L., & Samet, J. M. (2007). Spatial and Temporal Variation in PM2.5 Chemical Composition in the United States for Health Effects Studies. *Environmental Health Perspectives*, *115*(7), 989–995. https://doi.org/10.1289/ehp.9621

Brusselen, D. V., Oñate, W. A. de, Maiheu, B., Vranckx, S., Lefebvre, W., Janssen, S., … Avonts, D. (2016). Health Impact Assessment of a Predicted Air Quality Change by Moving Traffic from an Urban Ring Road into a Tunnel. The Case of Antwerp, Belgium. *PLOS ONE*, *11*(5), e0154052. https://doi.org/10.1371/journal.pone.0154052

Cains, T., Cannata, S., Ressler, K.-A., Sheppeard, V., & Ferson, M. (2003). *M5 East Tunnels Air Quality Monitoring Project*. South Eastern Sydney Public Health Unit & NSW Department of Health.

Central Transportation Planning Staff. (2011, March). I-93/Central Artery Between Columbia Road, Dorchester, and Route 1, Charlestown. Boston Region Metropolitan Planning Organization. Retrieved from ftp://ctps.org/pub/Express_Highway_Volumes/20_I93_Central_Artery.pdf

Central Transportation Planning Staff Geoserver. (2012). Traffic Counts on the Central Artery. Retrieved May 6, 2012, from ftp://ctps.org/pub/Express_Highway_Volumes/20_I93_Central_ Artery.pdf

Cheng, Y., Lee, S. C., Ho, K. F., & Louie, P. K. K. (2006). On-road particulate matter (PM2.5) and gaseous emissions in the Shing Mun Tunnel, Hong Kong. *Atmospheric Environment*, *40*(23), 4235–4245. https://doi.org/10.1016/j.atmosenv.2006.04.002

Chung, C.-Y., & Chung, P.-L. (2007). A numerical and experimental study of pollutant dispersion in a traffic tunnel. *Environmental Monitoring and Assessment*, *130*(1-3), 289–299. https://doi.org/10.1007/s10661-006-9397-0

Cimorelli, A. J., Steven G. Perry, Akula Venkatram, Jeffrey C. Weil, Robert J. Paine, Robert B. Wilson, … James O. Paumier. (2004, September). AERMOD-Description of Model Formulation. U.S. Environmental Protection Agency.

Colberg, C. A., Tona, B., Stahel, W. A., Meier, M., & Staehelin, J. (2005). Comparison of a road traffic emission model (HBEFA) with emissions derived from measurements in the Gubrist road tunnel, Switzerland. *Atmospheric Environment*, *39*(26), 4703–4714. https://doi.org/10.1016/j.atmosenv.2005.04.020

Cook, R., Isakov, V., Touma, J. S., Benjey, W., Thurman, J., Kinnee, E., & Ensley, D. (2008). Resolving local-scale emissions for modeling air quality near roadways. *Journal of the Air & Waste Management Association (1995)*, *58*(3), 451–461.

Deng, Y., Chen, C., Li, Q., Hu, Q., Yuan, H., Li, J., & Li, Y. (2015). Measurements of real-world vehicle CO and NOx fleet average emissions in urban tunnels of two cities in China. *Atmospheric Environment*, *122*, 417–426. https://doi.org/10.1016/j.atmosenv.2015.08.036

Eftekharian, E., Dastan, A., Abouali, O., Meigolinedjad, J., & Ahmadi, G. (2014). A numerical investigation into the performance of two types of jet fans in ventilation of an urban tunnel under traffic jam condition. *Tunnelling and Underground Space Technology*, *44*, 56–67. https://doi.org/10.1016/j.tust.2014.07.005

El-Fadel, M., & Hashisho, Z. (2001). Vehicular Emissions in Roadway Tunnels: A Critical Review. *Critical Reviews in Environmental Science and Technology*, *31*(2), 125–174. https://doi.org/10.1080/20016491089190

Engel-Cox, J. A., & Weber, S. A. (2007). Compilation and assessment of recent positive matrix factorization and UNMIX receptor model studies on fine particulate matter source apportionment for the eastern United States. *Journal of the Air & Waste Management Association (1995)*, *57*(11), 1307–1316.

Environmental Resources Management. (2015). *Air Quality Modeling Analysis*. Malvern, PA. Retrieved from https://www3.epa.gov/ttn/scram/guidance/mch/new_mch/15-II-01_Corning_Diesel_Mfg_Final_Modeling_Report_May2015.pdf

Franchini, M., & Mannucci, P. M. (2007). Short-term effects of air pollution on cardiovascular diseases: outcomes and mechanisms. *Journal of Thrombosis and Haemostasis: JTH*, *5*(11), 2169–2174. https://doi.org/10.1111/j.1538-7836.2007.02750.x

Fuller, C. H., Brugge, D., Williams, P. L., Mittleman, M. A., Durant, J. L., & Spengler, J. D. (2012). Estimation of ultrafine particle concentrations at near-highway residences using data from local and central monitors. *Atmospheric Environment*, *57*, 257–265. https://doi.org/10.1016/j.atmosenv.2012.04.004

Gao, P. Z., Liu, S. L., Chow, W. K., & Fong, N. K. (2004). Large eddy simulations for studying tunnel smoke ventilation. *Tunnelling and Underground Space Technology*, *19*(6), 577–586. https://doi.org/10.1016/j.tust.2004.01.005

Gertler, A., Gillies, J. A., Pierson, W. R., Rogers, F. C., Sagebiel, J. C., Abu-Allaban, M., … Cahill, T. A. (2002, January). Emissions from Diesel and Gasoline Engines Measured in Highway Tunnels. Retrieved May 9, 2017, from https://www.healtheffects.org/publication/emissions-diesel-and-gasoline-engines-measured-highway-tunnels

Gidhagen, L., Johansson, C., Ström, J., Kristensson, A., Swietlicki, E., Pirjola, L., & Hansson, H.-C. (2003). Model simulation of ultrafine particles inside a road tunnel. *Atmospheric Environment*, *37*(15), 2023–2036. https://doi.org/10.1016/S1352-2310(03)00124-9

Gillies, J. A., Gertler, A. W., Sagebiel, J. C., & Dippel, W. A. (2001). On-Road Particulate Matter (PM2.5 and PM10) Emissions in the Sepulveda Tunnel, Los Angeles, California. *Environmental Science & Technology*, *35*(6), 1054–1063. https://doi.org/10.1021/es991320p

Ginzburg, H., Liu, X., Baker, M., Shreeve, R., Jayanty, R. K. M., Campbell, D., & Zielinska, B. (2015). Monitoring study of the near-road PM2.5 concentrations in Maryland. *Journal of the Air & Waste Management Association (1995)*, *65*(9), 1062–1071. https://doi.org/10.1080/10962247.2015.1056887

Ginzburg, H., & Schattanek, G. (1997). Analytical Approach to Estimate Pollutant Concentrations from a Tunnel Portal Exit Plume. Retrieved from https://www.osti.gov/scitech/biblio/351682

Grieshop, A. P., Lipsky, E. M., Pekney, N. J., Takahama, S., & Robinson, A. L. (2006). Fine particle emission factors from vehicles in a highway tunnel: Effects of fleet composition

and season. *Atmospheric Environment*, *40, Supplement 2*, 287–298. https://doi.org/10.1016/j.atmosenv.2006.03.064

Handler, M., Puls, C., Zbiral, J., Marr, I., Puxbaum, H., & Limbeck, A. (2008). Size and composition of particulate emissions from motor vehicles in the Kaisermühlen-Tunnel, Vienna. *Atmospheric Environment*, *42*(9), 2173–2186. https://doi.org/10.1016/j.atmosenv.2007.11.054

Harrison, R. M., & Yin, J. (2000). Particulate matter in the atmosphere: which particle properties are important for its effects on health? *Science of The Total Environment*, *249*(1–3), 85–101. https://doi.org/10.1016/S0048-9697(99)00513-6

Isakov, V., Arunachalam, S., Batterman, S., Bereznicki, S., Burke, J., Dionisio, K., … Vette, A. (2014). Air Quality Modeling in Support of the Near-Road Exposures and Effects of Urban Air Pollutants Study (NEXUS). *International Journal of Environmental Research and Public Health*, *11*(9), 8777–8793. https://doi.org/10.3390/ijerph110908777

Ito, K., Xue, N., & Thurston, G. (2004). Spatial variation of PM2.5 chemical species and source-apportioned mass concentrations in New York City. *Atmospheric Environment*, *38*(31), 5269–5282. https://doi.org/10.1016/j.atmosenv.2004.02.063

Kheirbek, I., Haney, J., Douglas, S., Ito, K., & Matte, T. (2016). The contribution of motor vehicle emissions to ambient fine particulate matter public health impacts in New York City: a health burden assessment. *Environmental Health*, *15*, 89. https://doi.org/10.1186/s12940-016-0172-6

Lakes Environmental. (2017). AERMOD View. Retrieved May 4, 2017, from https://www.weblakes.com/products/aermod/

Lall, R., & Thurston, G. D. (2006). Identifying and quantifying transported vs. local sources of New York City PM2.5 fine particulate matter air pollution. *Atmospheric Environment*, *40, Supplement 2*, 333–346. https://doi.org/10.1016/j.atmosenv.2006.04.068

Lee, H. J., Gent, J. F., Leaderer, B. P., & Koutrakis, P. (2011a). Spatial and temporal variability of fine particle composition and source types in five cities of Connecticut and Massachusetts. *The Science of the Total Environment*, *409*(11), 2133–2142. https://doi.org/10.1016/j.scitotenv.2011.02.025

Lee, H. J., Liu, Y., Coull, B. A., Schwartz, J., & Koutrakis, P. (2011b). A novel calibration approach of MODIS AOD data to predict PM2.5 concentrations. *Atmos. Chem. Phys.*, *11*(15), 7991–8002. https://doi.org/10.5194/acp-11-7991-2011

Lepage M, Vanderheyden M, Davies A. (1997). Evaluating ambient air quality at exit portals of the Central /Artery Tunnel - ScienceBase-Catalog. Retrieved January 12, 2017, from https://www.sciencebase.gov/catalog/item/5053a375e4b097cd4fce8d7c

MacNee, W., & Donaldson, K. (2003). Mechanism of lung injury caused by PM10 and ultrafine particles with special reference to COPD. *The European Respiratory Journal. Supplement*, *40*, 47s–51s.

Masri, S., Kang, C.-M., & Koutrakis, P. (2015). Composition and Sources of Fine and Coarse Particles Collected during 2002–2010 in Boston, MA. *Journal of the Air & Waste Management Association (1995)*, *65*(3), 287–297. https://doi.org/10.1080/10962247.2014.982307

Massachusetts Department of Transportation. (2013). Yearly Traffic & Revenue HIstory. Retrieved from https://www.massdot.state.ma.us/Portals/0/docs/infoCenter/financials/toll_reports/YearlyTrafficRevenue2013.pdf

Massachusetts Department of Transportation. (2017a). Project Background - The Big Dig - Highway Division. Retrieved February 25, 2017, from https://www.massdot.state.ma.us/highway/TheBigDig/ProjectBackground.aspx
Massachusetts Department of Transportation. (2017b). Tunnels & Bridges. Retrieved May 3, 2017, from https://www.massdot.state.ma.us/highway/TheBigDig/TunnelsBridges.aspx
MassGIS. (2014). MassGIS Data - Community Boundaries (Towns) [Mass.gov]. Retrieved March 24, 2017, from http://www.mass.gov/anf/research-and-tech/it-serv-and-support/application-serv/office-of-geographic-information-massgis/datalayers/towns.html
McGrath, T., Sorensen, A., Collyer, L., Webber, K., Webber, B., Dufour, K., & Keith, G. (2016). Massachusetts 2015 Air Quality Report. Massachusetts Department of Environmental Protection. Retrieved from http://www.mass.gov/eea/docs/dep/air/priorities/15aqrpt.pdf
Miao, S. J., & Fu, D. F. (2013). Case Study of Nanjing Inner Ring on Air Pollution Dispersion from Roadway Tunnel Portals. *Advanced Materials Research*, *610-613*, 1895–1900. https://doi.org/10.4028/www.scientific.net/AMR.610-613.1895
Michanowicz, D. R., Shmool, J. L. C., Tunno, B. J., Tripathy, S., Gillooly, S., Kinnee, E., & Clougherty, J. E. (2016). A hybrid land use regression/AERMOD model for predicting intra-urban variation in PM2.5. *Atmospheric Environment*, *131*, 307–315. https://doi.org/10.1016/j.atmosenv.2016.01.045
Milando, C. (2012, May 10). *Seasonal Variation of Emission Factors for Ultrafine Particles from On-Highway Vehicles*. Tufts University, School of Engineering, Medford, Massachusetts.
Missouri Department of Natural Resources. (2013, November 12). Building Downwash & Good Engineering Practice Stack Height. Retrieved from http://dnr.mo.gov/env/apcp/docs/bldgdownwashandgep10-29-12.pdf
Nadel, C. B., & Vanderheyden, M. D. (2000). Relationships for Determining the Dispersion of Portal Emissions from One-Way Roadway Tunnels. Presented at the 10th International Symposium on Aerodynamics and Ventilation of Vehicle Tunnels- Principles, Analysis and Design, Held Boston, USA, 1-3 November 2000. Retrieved from https://trid.trb.org/view.aspx?id=709958
NAVTEQ Traffic. (2012). Retrieved from http://stakeholder.traffic.com/mainmenu/stakeholder.html
NOAA. (n.d.). Land-Based Station Data. Retrieved March 25, 2017, from https://www.ncdc.noaa.gov/data-access/land-based-station-data
NOAA, Earth System Research Laboratory, & Global Systems Division. (2016, January). NOAA/ESRL Radiosonde Database. Retrieved March 25, 2017, from https://esrl.noaa.gov/raobs/
Oettl, D. (2015). Quality assurance of the prognostic, microscale wind-field model GRAL 14.8 using wind-tunnel data provided by the German VDI guideline 3783-9. *Journal of Wind Engineering and Industrial Aerodynamics*, *142*, 104–110. https://doi.org/10.1016/j.jweia.2015.03.014
Oettl, D., Sturm, P., Almbauer, R., Okamoto, S., & Horiuchi, K. (2003). Dispersion from road tunnel portals: comparison of two different modelling approaches. *Atmospheric Environment*, *37*(37), 5165–5175. https://doi.org/10.1016/j.atmosenv.2003.09.003
Oettl, D., Sturm, P. J., Bacher, M., Pretterhofer, G., & Almbauer, R. A. (2002). A simple model for the dispersion of pollutants from a road tunnel portal. *Atmospheric Environment*, *36*(18), 2943–2953. https://doi.org/10.1016/S1352-2310(02)00254-6

Okamoto, S., Sakai, K., Matsumoto, K., Horiuchi, K., & Kobayashi, K. (1998). Development and Application of a Three-Dimensional Taylor–Galerkin Numerical Model for Air Quality Simulation near Roadway Tunnel Portals. *Journal of Applied Meteorology*, *37*(10), 1010–1025. https://doi.org/10.1175/1520-0450(1998)037<1010:DAAOAT>2.0.CO;2

Orru, H., Lövenheim, B., Johansson, C., & Forsberg, B. (2015). Potential health impacts of changes in air pollution exposure associated with moving traffic into a road tunnel. *Journal of Exposure Science & Environmental Epidemiology*, *25*(5), 524–531. https://doi.org/10.1038/jes.2015.24

Padró-Martínez, L. T., Patton, A. P., Trull, J. B., Zamore, W., Brugge, D., & Durant, J. L. (2012). Mobile monitoring of particle number concentration and other traffic-related air pollutants in a near-highway neighborhood over the course of a year. *Atmospheric Environment*, *61*, 253–264. https://doi.org/10.1016/j.atmosenv.2012.06.088

Patton, A. P., Perkins, J., Zamore, W., Levy, J. I., Brugge, D., & Durant, J. L. (2014). Spatial and temporal differences in traffic-related air pollution in three urban neighborhoods near an interstate highway. *Atmospheric Environment*, *99*, 309–321. https://doi.org/10.1016/j.atmosenv.2014.09.072

Perkins, J. L., Padró-Martínez, L. T., & Durant, J. L. (2013). Particle number emission factors for an urban highway tunnel. *Atmospheric Environment*, *74*, 326–337. https://doi.org/10.1016/j.atmosenv.2013.03.046

Perry, S. G., Heist, D. K., Brouwer, L. H., Monbureau, E. M., & Brixey, L. A. (2016). Characterization of pollutant dispersion near elongated buildings based on wind tunnel simulations. *Atmospheric Environment*, *142*, 286–295. https://doi.org/10.1016/j.atmosenv.2016.07.052

Riedl, M. A. (2008). The effect of air pollution on asthma and allergy. *Current Allergy and Asthma Reports*, *8*(2), 139–146.

Rowangould, G. M. (2015). A new approach for evaluating regional exposure to particulate matter emissions from motor vehicles. *Transportation Research Part D: Transport and Environment*, *34*, 307–317. https://doi.org/10.1016/j.trd.2014.11.020

Seaton, A., Godden, D., MacNee, W., & Donaldson, K. (1995). Particulate air pollution and acute health effects. *The Lancet*, *345*(8943), 176–178. https://doi.org/10.1016/S0140-6736(95)90173-6

Squizzato, S., Cazzaro, M., Innocente, E., Visin, F., Hopke, P. K., & Rampazzo, G. (2017). Urban air quality in a mid-size city — PM2.5 composition, sources and identification of impact areas: From local to long range contributions. *Atmospheric Research*, *186*, 51–62. https://doi.org/10.1016/j.atmosres.2016.11.011

The Massachusetts Department of Transportation- Office of Transportation Planning,. (2014). MassGIS Data - MassDOT Roads [Mass.gov]. Retrieved March 24, 2017, from http://www.mass.gov/anf/research-and-tech/it-serv-and-support/application-serv/office-of-geographic-information-massgis/datalayers/eotroads.html

TRC/Parsons Brinckerhoff. (2012, August 1). Central Artery (I-93)/Tunnel (I-90) Project: Operating Certification of the Project Ventilation System. Retrieved from http://www.mass.gov/eea/agencies/massdep/air/reports/operating-certification-central-artery-tunnel-ventilation-system.html

US EPA. (2005, November 9). 40 CFR Appendix W to Part 51 - Guideline on Air Quality Models. Retrieved November 16, 2016, from https://www.gpo.gov/fdsys/granule/CFR-2011-title40-vol2/CFR-2011-title40-vol2-part51-appW

US EPA. (2010, June 22). Pt. 53, Subpt C, Table C-4. Retrieved from https://www.gpo.gov/fdsys/pkg/CFR-2015-title40-vol6/pdf/CFR-2015-title40-vol6-part53-subpartC-appC-id49.pdf

US EPA. (2016a, December 20). NAAQS Table [Policies and Guidance]. Retrieved April 24, 2017, from https://www.epa.gov/criteria-air-pollutants/naaqs-table

US EPA. (2016b, December 23). Pre-Generated Data Files [Data & Tools]. Retrieved March 25, 2017, from https://aqsdr1.epa.gov/aqsweb/aqstmp/airdata/download_files.html

US EPA. (2017, April 24). Sampling Methods for PM2.5 Speciation parameters. Retrieved April 24, 2017, from https://aqs.epa.gov/aqsweb/documents/codetables/methods_speciation.html

U.S. Government Publishing Office. Code of Federal Regulations, 40 CFR Part 58 § Appendix A-3 (2016). Retrieved from https://www.ecfr.gov/cgi-bin/text-idx?SID=20634c28300ba7afb67db98abcd2961d&node=ap40.6.58_161.a&rgn=div9

Valavanidis, A., Fiotakis, K., & Vlachogianni, T. (2008). Airborne particulate matter and human health: toxicological assessment and importance of size and composition of particles for oxidative damage and carcinogenic mechanisms. *Journal of Environmental Science and Health. Part C, Environmental Carcinogenesis & Ecotoxicology Reviews*, *26*(4), 339–362. https://doi.org/10.1080/10590500802494538

Weingartner, E., Keller, C., Stahel, W. A., Burtscher, H., & Baltensperger, U. (1997). Aerosol emission in a road tunnel. *Atmospheric Environment*, *31*(3), 451–462. https://doi.org/10.1016/S1352-2310(96)00193-8

W. Kirchstetter, T., Harley, R. A., Kreisberg, N. M., Stolzenburg, M. R., & Hering, S. V. (1999). On-road measurement of fine particle and nitrogen oxide emissions from light- and heavy-duty motor vehicles. *Atmospheric Environment*, *33*(18), 2955–2968. https://doi.org/10.1016/S1352-2310(99)00089-8

Yura, E. A., Kear, T., & Niemeier, D. (2007). Using CALINE dispersion to assess vehicular PM2.5 emissions. *Atmospheric Environment*, *41*(38), 8747–8757. https://doi.org/10.1016/j.atmosenv.2007.07.045

Zhou, R., Wang, S., Shi, C., Wang, W., Zhao, H., Liu, R., … Zhou, B. (2014). Study on the Traffic Air Pollution inside and outside a Road Tunnel in Shanghai, China. *PLOS ONE*, *9*(11), e112195. https://doi.org/10.1371/journal.pone.0112195

Appendix

Appendix A. Figures

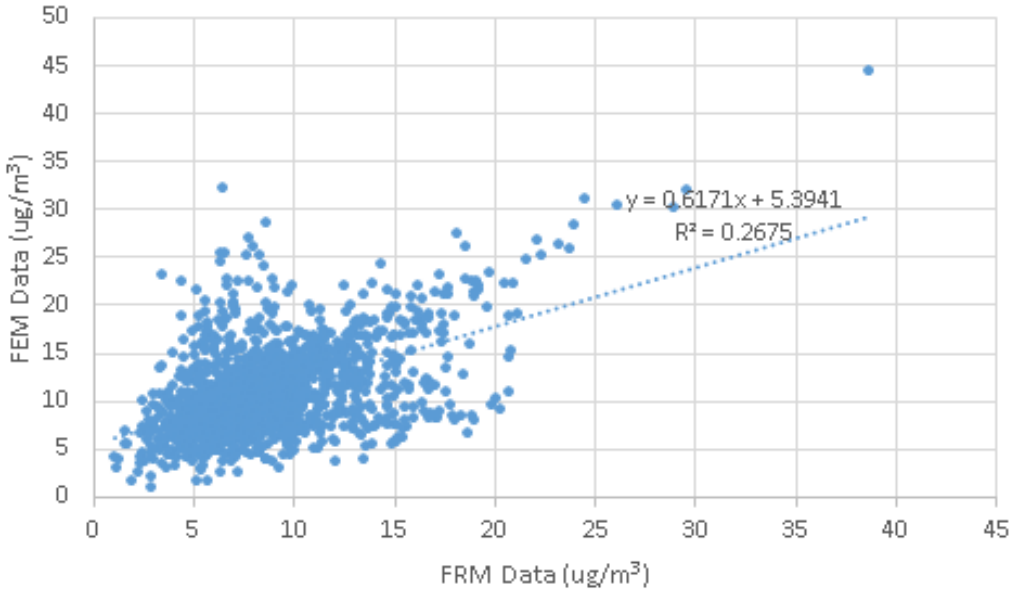

Figure A.1 FEM versus FRM data at the North Street site (#25-025-0043) for 2011–2015.

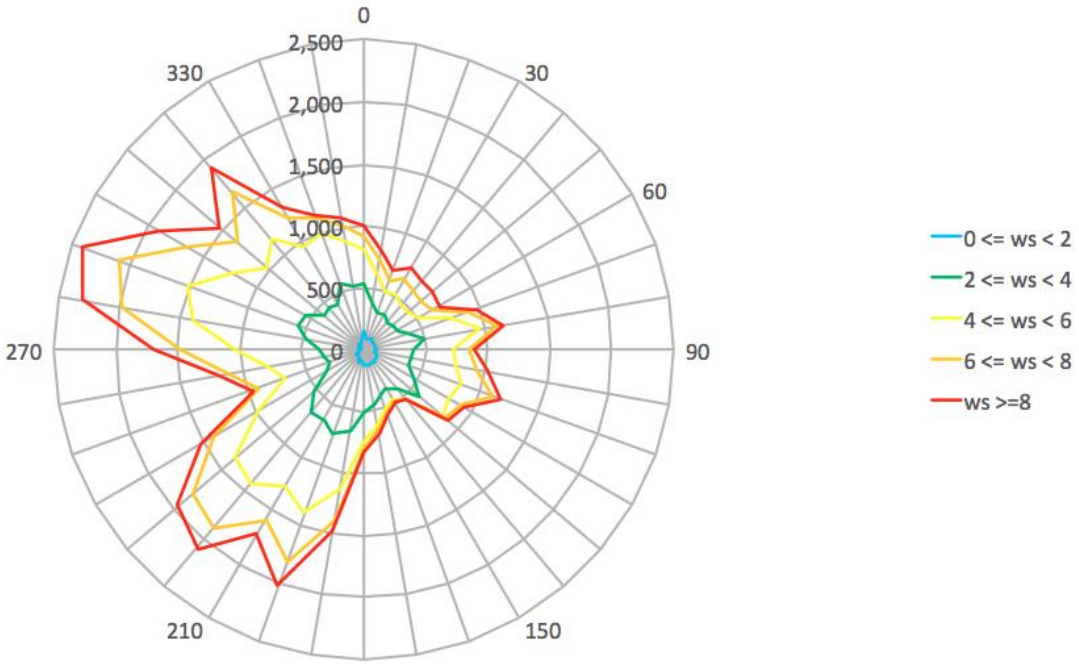

Figure A.2 Annual Wind Rose from Logan Airport (Station #14739) for 2011–2015 where the y-axis is the cumulative number of hours measured in each 10-degree wind bin.

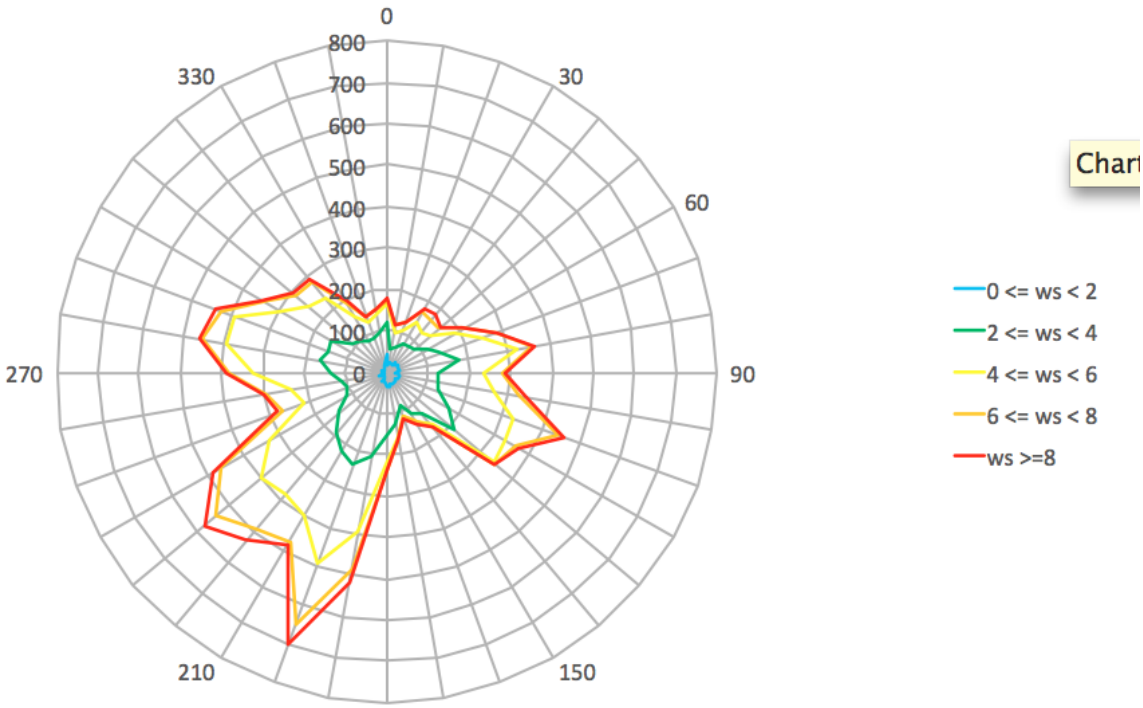

Figure A.3 Summer (June, July, August) Wind Rose from Logan Airport (Station #14739) for 2011–2015 where the y-axis is the cumulative number of hours measured in each 10-degree wind bin.

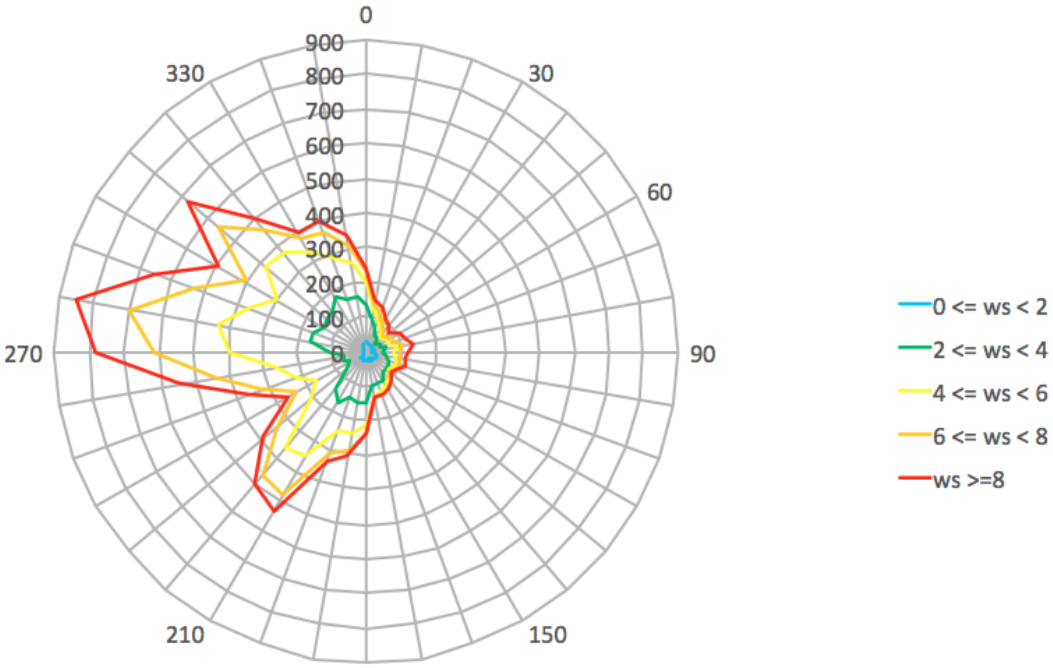

Figure A.4 Winter (December, January, February) Wind Rose from Logan Airport (Station #14739) for 2011–2015 where the y-axis is the cumulative number of hours measured in each 10-degree wind bin.

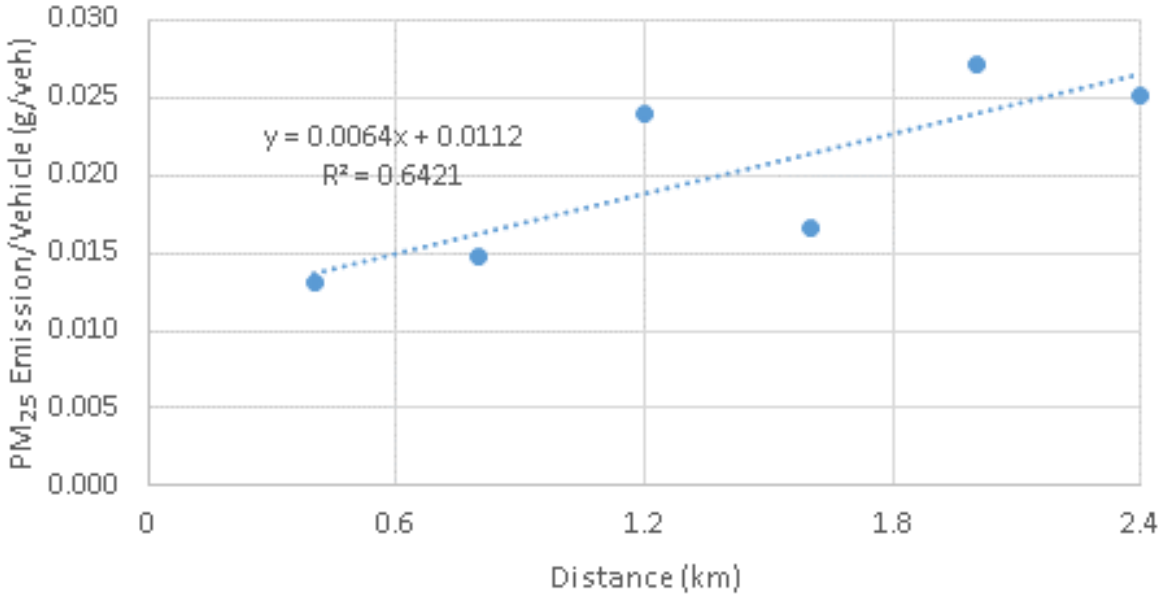

Figure A.5 $PM_{2.5}$ Emission Factor per Vehicle (grams per vehicle) compared to Distance through the Tunnel (kilometers) for January 6, 2011.

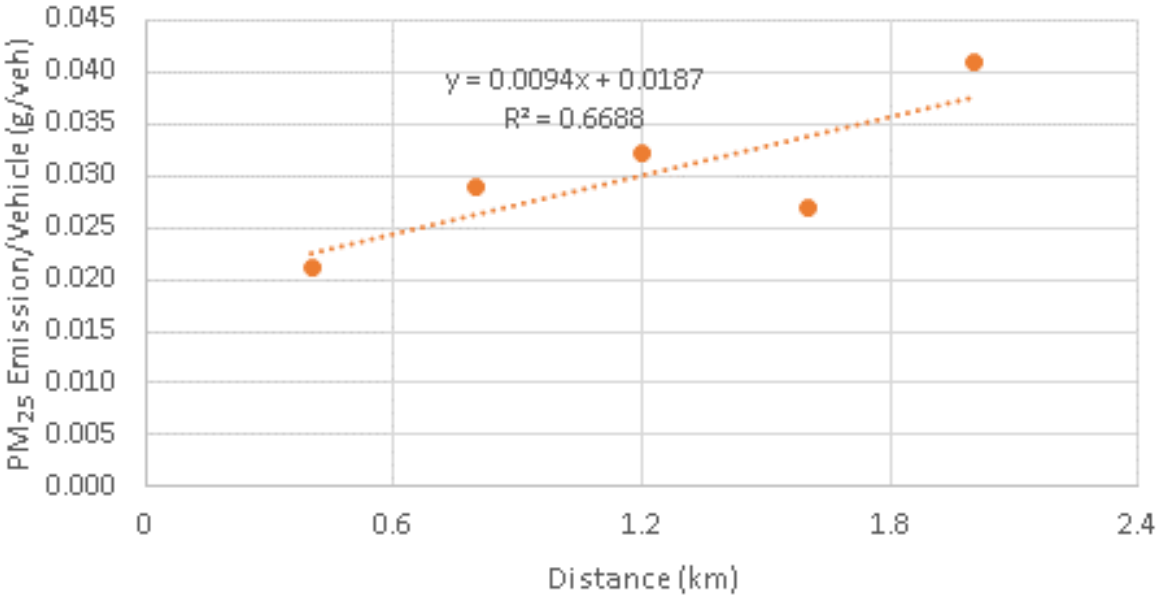

Figure A.6 $PM_{2.5}$ Emission Factor per Vehicle (grams per vehicle) compared to Distance through the Tunnel (kilometers) for January 11, 2011.

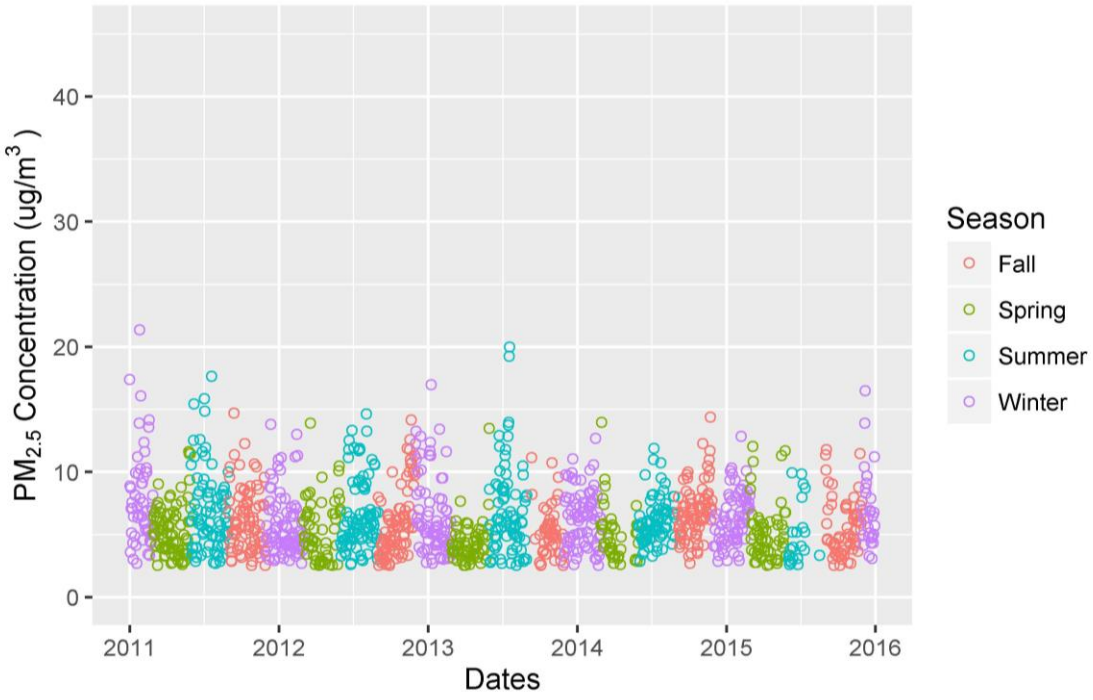

Figure A.7. $PM_{2.5}$ FEM Concentration at the Blue Hill Observatory (#25-021-3003) by Season for 2011–2015. Seasons: Winter (December, January, February), Spring (March, April, May), Summer (June, July, August), Fall (September, October, November)

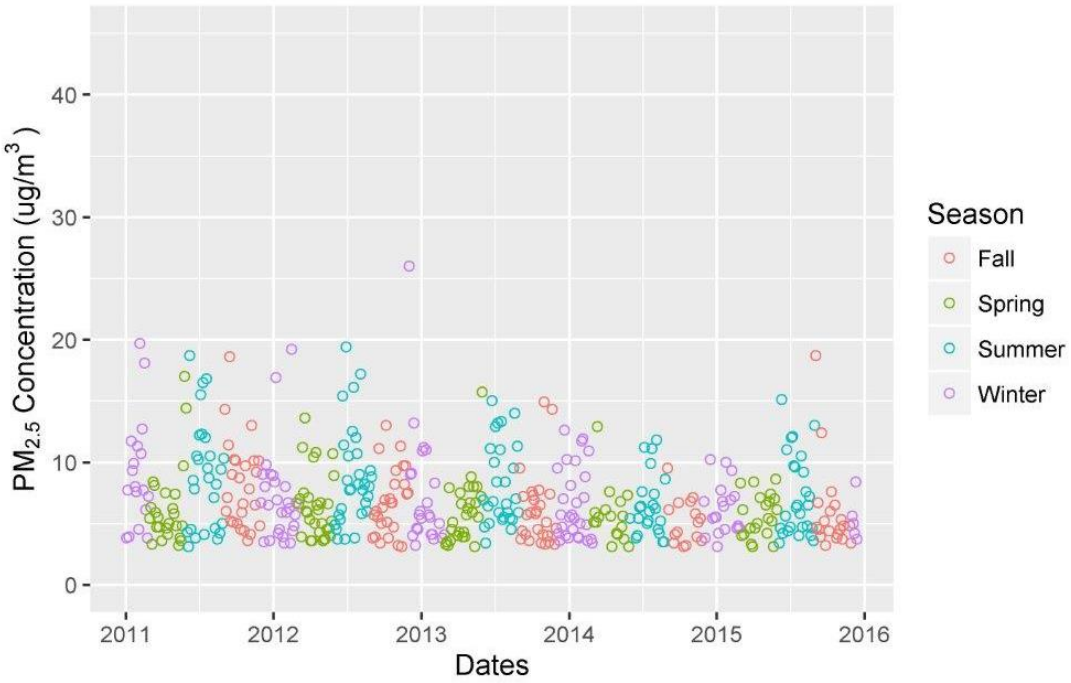

Figure A.8. $PM_{2.5}$ FRM Concentration at Lynn (#25-009-2006) by Season for 2011–2015. Seasons: Winter (December, January, February), Spring (March, April, May), Summer (June, July, August), Fall (September, October, November).

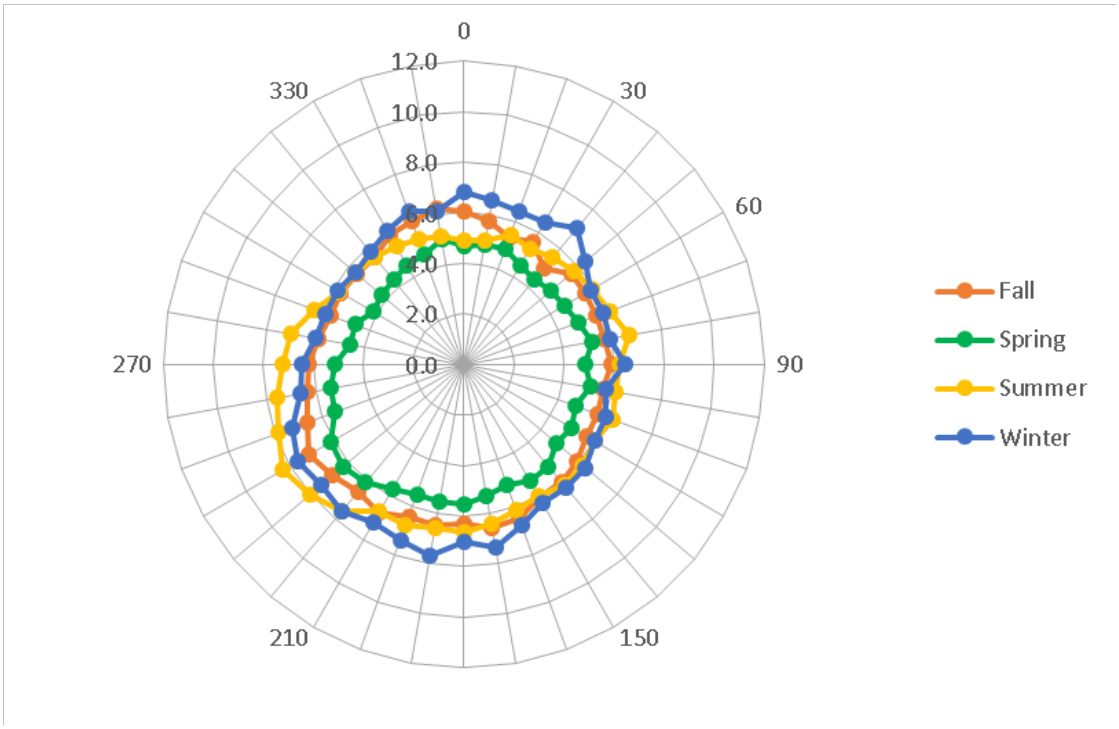

Figure A.9. Seasonal $PM_{2.5}$ Concentration Rose of Ten-Degree Averaged Wind Bins at the Blue Hill Observatory (#25-021-3003) for 2011–2015. Seasons: Winter (December, January, February), Spring (March, April, May), Summer (June, July, August), Fall (September, October, November).

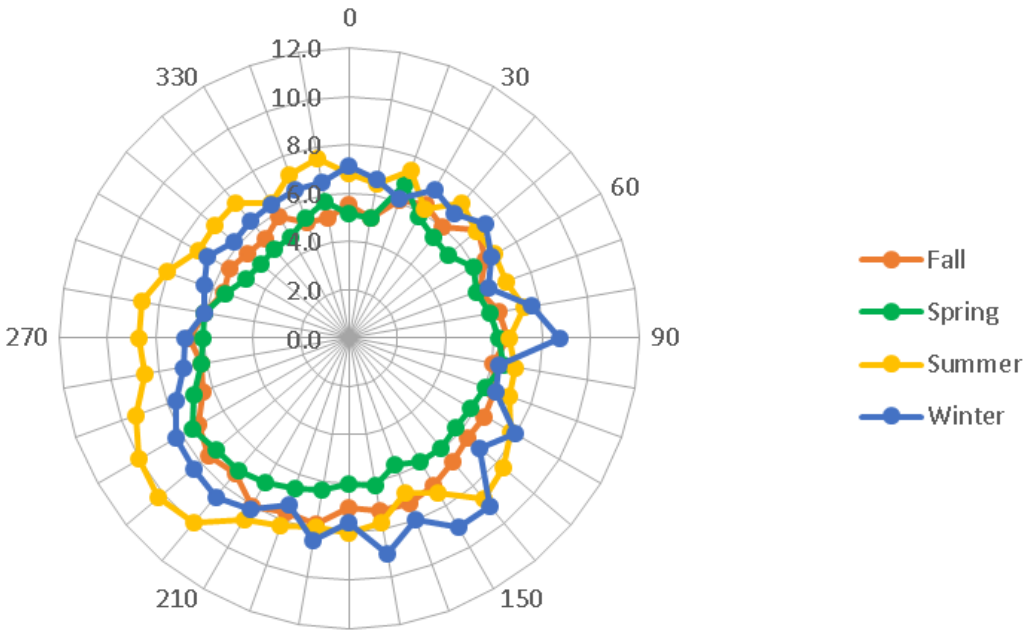

Figure A.10. Seasonal $PM_{2.5}$ Concentration Rose of Ten-Degree Averaged Wind Bins at Lynn (#25-009-2006) for 2011–2015. Seasons: Winter (December, January, February), Spring (March, April, May), Summer (June, July, August), Fall (September, October, November).

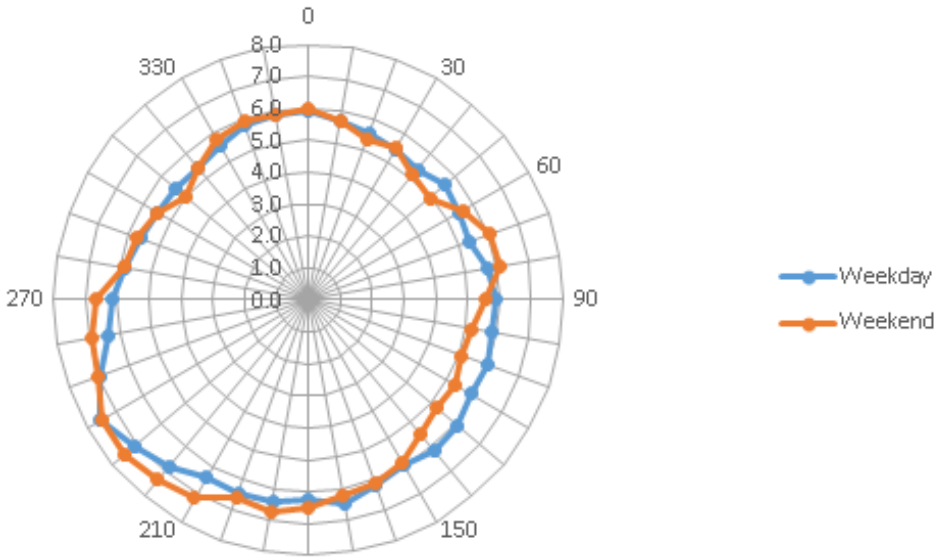

Figure A.11. Weekend and Weekday Adjusted $PM_{2.5}$ Concentration Rose of Ten-Degree Averaged Wind Bins at the Blue Hill Observatory (#25-021-3003) for 2011–2015. Classifications: Weekends (Saturday, Sunday), Weekdays (Monday, Tuesday, Wednesday, Thursday, Friday).

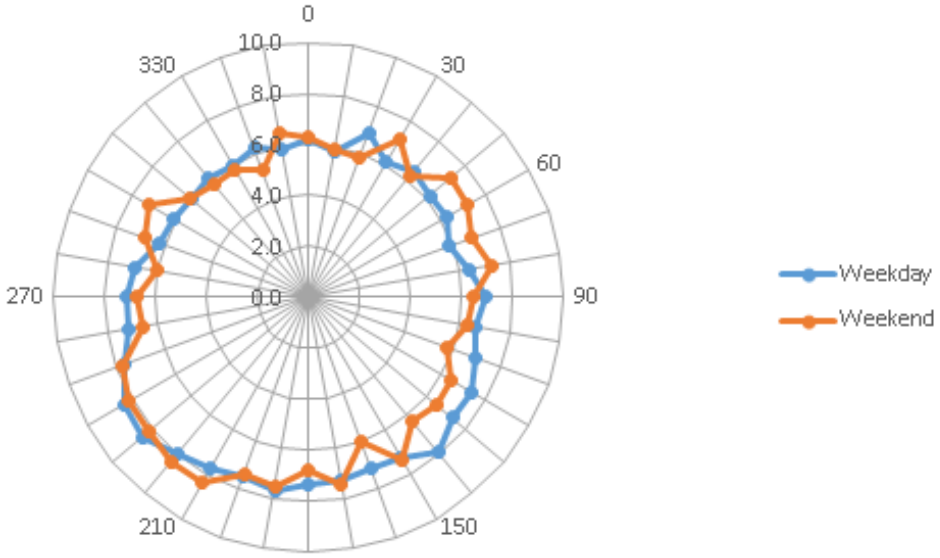

Figure A.12. Weekend and Weekday FRM $PM_{2.5}$ Concentration Rose of Ten-Degree Averaged Wind Bins at Lynn (#25-009-2006) for 2011–2015. Classifications: Weekends (Saturday, Sunday), Weekdays (Monday, Tuesday, Wednesday, Thursday, Friday).